

THE VERY LARGE ARRAY OBSERVATIONAL STATUS SUMMARY

Edited by J.S. Ulvestad, R.A. Perley, & C.J. Chandler

January 15, 2009

Contents

1	INTRODUCTION	4
1.1	Purpose of Document	4
1.2	What is the Expanded VLA?	4
1.3	VLA to EVLA Transition	4
2	AN OVERVIEW OF THE VLA	6
3	PERFORMANCE OF THE VLA	8
3.1	Resolution	8
3.2	Sensitivity	9
3.3	EVLA Frequency Bands and Tunability	15
3.4	Elevation Effects	16
3.5	Field of View	21
3.5.1	Primary Beam	21
3.5.2	Chromatic Aberration (Bandwidth Smearing)	22
3.5.3	Time-Averaging Loss	22
3.5.4	Non-Coplanar Baselines	23
3.6	Time Resolution	23
3.7	Radio-Frequency Interference	24
3.8	Antenna Pointing	29
3.9	Subarrays	29
3.10	Positional Accuracy	30
3.11	Limitations on Imaging Performance	30
3.11.1	Image Fidelity	31
3.11.2	VLA-EVLA Closure Errors	31
3.11.3	Invisible Structures	31
3.11.4	Poorly Sampled Fourier Plane	32
3.11.5	Sidelobes from Confusing Sources	32
3.11.6	Sidelobes from Strong Sources	32
3.12	Calibration and the Flux Density Scale	32
3.13	Phase Calibration	34
3.13.1	General Guidelines for Phase Calibration	34
3.13.2	Rapid Phase Calibration and the Atmospheric Phase Interferometer (API)	34

3.14	Polarization	35
3.15	Spectral Line Modes	36
3.16	VLBI Observations	39
3.17	Snapshots	40
3.18	Shadowing and Cross-Talk	40
3.19	Combining Configurations and Mosaicing	40
3.20	Pulsar Observing	41
3.21	Observing High Flux Density Sources – Special Corrections	41
3.22	Using VLA and EVLA Antennas Together	41
4	USING THE VLA	41
4.1	Obtaining Observing Time on the VLA	41
4.2	Rapid Response Science	42
4.3	Data Analysts and General Assistance	43
4.4	Observing File Preparation	43
4.5	Fixed Date and Dynamic Scheduling	44
4.6	The Observations and Remote Observing	44
4.7	Data Processing	44
4.8	Travel Support for Visiting the DSOC and VLA	45
4.9	Student Assistance for Data Reduction Visits to the DSOC	45
4.10	Real-Time Observing	45
4.11	Computing at the DSOC	46
4.12	Reservations for VLA and/or DSOC	46
4.13	Staying in Socorro	46
4.14	Help for Visitors to the VLA and DSOC	46
4.15	VLBI Remote Observing	47
4.16	On-Line Information about the NRAO and the VLA	47
5	MISCELLANEOUS	47
5.1	VLA Archive Data	47
5.2	Publication Guidelines	47
5.2.1	Acknowledgement to NRAO	47
5.2.2	Dissertations	48
5.2.3	Preprints	48
5.2.4	Reprints	48
5.2.5	Page Charge Support	48
6	DOCUMENTATION	49
7	KEY PERSONNEL	50
8	Acknowledgments	50

List of Tables

1	Overall EVLA Performance Goals	5
2	EVLA Major Milestones	5
3	Predicted VLA Configuration Schedule for 2009–2010	7

4	Configuration Properties	10
5	VLA Sensitivity in Mid-2009	11
6	EVLA Sensitivity Goals	12
7	Sensitivity Ranges of VLA Bands	14
8	Tuning Ranges of EVLA Bands	17
9	Average Power Gain Coefficients for the VLA Antennas	19
10	Average Inverse Voltage Gain Coefficients for the VLA Antennas	20
11	Reduction in Peak Response Due to Bandwidth Smearing	22
12	Loss vs. Averaging Time for Time Averaging Smearing	23
13	Minimum Integration Times for One Subarray of 27 Antennas	24
14	VLA RFI Between 1260 and 1740 MHz	26
15	Recommended Center Frequency/Bandwidth Combinations for L band	27
16	Jobserve Names of L band ‘Standard Frequencies’	28
17	Flux Densities (Jy) of Standard Calibrators for November 2001	33
18	Available Bandwidths and Numbers of Spectral Line Channels in Normal Mode	37
19	Available Bandwidths and Numbers of Spectral Line Channels in Hanning Smoothing Mode	38
20	Key VLA Personnel	51

List of Figures

1	System Temperatures vs. Frequency at K and Q Bands	13
2	VLA Sensitivity Between 1150 and 1250 MHz	15
3	EVLA Receiver Deployment Plan	16
4	Low-frequency Receiver Availability	17
5	High-frequency Receiver Availability	18
6	Ka-band sensitivity as a function of frequency	19
7	System Temperature Variations with Elevation at L, K, and Q Bands	20
8	EVLA System Temperature Variation with Elevation at L Band	21
9	Typical L-band Interference Spectrum	25
10	Typical P-band Interference Spectrum	25

1 INTRODUCTION

1.1 Purpose of Document

This document summarizes the current instrumental status of the Very Large Array. It is intended as a ready reference for those contemplating use of the VLA for their astronomical research. The information is in summary form – those requiring greater detail should consult the VLA’s staff members, listed in Section 7, or refer to the manuals and documentation listed in Section 6. Most of the information contained here, and much more, is available on the Web, and can be accessed through the VLA home page information for astronomers, at <http://www.vla.nrao.edu/astro/>. A companion document for the VLBA is also available from <http://www.vlba.nrao.edu/astro/>.

The Very Large Array is a large and complex modern instrument. It cannot be treated as a ‘black box’, and some familiarity with the principles and practices of its operation is necessary before efficient use can be made of it. Although the NRAO strives to make using the VLA as simple as possible, users must be aware that proper selection of observing mode and calibration technique is often crucial to the success of an observing program. Inexperienced and first-time users are especially encouraged to enlist the assistance of an experienced colleague or NRAO staff member for advice on, or direct participation in, an observing program. Refer to Section 4.14 for details. The VLA is an extremely flexible instrument, and we are always interested in imaginative and innovative ways of using it.

1.2 What is the Expanded VLA?

The Expanded VLA, or EVLA, is the product of a program to modernize the electronics of the VLA in order to improve several key observational parameters by an order of magnitude or more. Some of the details of the EVLA Project may be found on the web, at <http://www.aoc.nrao.edu/evla/>. The EVLA is funded jointly by the US National Science Foundation (NSF), the Canadian National Research Council, and the CONACyT funding agency in Mexico. Total funding is approximately \$94 million in Year 2005 dollars, including \$59 million in new NSF funding, \$16 million in redistributed effort from the NRAO Operations budget, \$17 million for the correlator from Canada, and \$2 million from Mexico. The EVLA project will be completed on time and on budget in 2012, 11 years after it began. Its key observational goals are (1) complete frequency coverage from 1 to 50 GHz; (2) sensitivity improvement by up to an order of magnitude (nearly two orders of magnitude in speed) by increasing the bandwidth from 100 MHz per polarization to 8 GHz per polarization; and (3) implementation of a new correlator that can process the large bandwidth with a minimum of 16,384 spectral channels per baseline. A comparison of some of the EVLA performance parameters to those of the VLA is provided in Table 1.

The remaining major milestones for the EVLA are shown in Table 2.

1.3 VLA to EVLA Transition

The years 2009 and 2010 will see a dramatic ramp-up in commissioning activities for the EVLA. This will mark the changeover from the “old” VLA, based on analog data transmission to the original VLA correlator, to the “new” EVLA, based on digital data transmission to the new EVLA correlator supplied by the Canadian Herzberg Institute of Astrophysics. During the entire EVLA implementation, we are committed to keeping the VLA observing and producing forefront science. However, this necessitates some compromises, such as

Table 1: **Overall EVLA Performance Goals**

Parameter	VLA	EVLA	Factor
Continuum Sensitivity ($1-\sigma$, 9 hr)	10 μ Jy	1 μ Jy	10
Maximum BW in each polarization	0.1 GHz	8 GHz	80
Number of frequency channels at max. BW	16	16,384	1024
Maximum number of freq. channels	512	4,194,304	8192
Coarsest frequency resolution	50 MHz	2 MHz	25
Finest frequency resolution	381 Hz	0.12 Hz	3180
Number of full-polarization sub-correlators	2	64	32
Log (Frequency Coverage over 1–50 GHz)	22%	100%	5

Note: The “Factor” gives the factor by which the EVLA parameter will be an improvement over the equivalent VLA parameter.

Table 2: **EVLA Major Milestones**

Milestone	Target Date
Complete testing of 4-station prototype correlator	Q1 2009
Full EVLA correlator installation	Q4 2009
Complete testing of 10-station correlator	Q1 2010
Decommission VLA correlator	Q1 2010
Shared Risk Observing begins	Q1 2010
Last antenna retrofitted	Q3 2010
Last receiver installed	Q3 2012

periods when the amount of observing time is reduced, and the average number of antennas available may be fewer than for the nominal VLA. The present document supplies a snapshot of the VLA capabilities and our expectations for the schedule of transition to the EVLA, as of the beginning of 2009. Prospective users *must* consult the up-to-date information provided on the web before proposing or undertaking VLA observations. In particular, impacts of the VLA-EVLA transition system on observers and their data reduction processes are summarized at <http://www.vla.nrao.edu/astro/guides/evlareturn/>. Short, medium, and long-term impact forecasts for the VLA-EVLA transition system also may be accessed directly from <http://www.vla.nrao.edu/astro/>.

We now are returning retrofitted EVLA antennas to the VLA to be used as part of normal VLA observations, at the rate of approximately one antenna every two months. At present, most of the antennas present in a VLA observation are these retrofitted EVLA systems. These antennas have new feed systems, wideband electronics, and fiber-optic data transmission systems; their data are “translated” (and reduced considerably) to be correlated against VLA antennas in the VLA correlator. Throughout this document, the term “EVLA antennas” will refer to those that have gone through this retrofit and now speak a digital language, whereas the term “VLA antennas” will refer to those antennas that have not yet gone through their digital retrofit. Although we have put considerable effort into making it possible to observe with mixed arrays of VLA and EVLA antennas, fundamental hardware differences (e.g., mismatched bandpasses) lead to a number of complications,

which often must be taken into account in constructing observing programs or in analyzing data. Some information is provided in this document about observations using VLA+EVLA antennas, but details change frequently; the web links indicated above *must* be consulted before VLA observations are undertaken.

2 AN OVERVIEW OF THE VLA

The VLA is a 27-element interferometric array, arranged along the arms of an upside-down “Y”, which will produce images of the radio sky at a wide range of frequencies and resolutions. It is located at an elevation of 2100 meters on the Plains of San Agustin in Southwestern New Mexico, and is managed from the Pete V. Domenici Science Operations Center (DSOC) in Socorro, New Mexico. **VLA users should note that 2009 and 2010 are key years in the transition from the original VLA to the Expanded VLA. The traditional VLA properties that are described in Sections 2 and 3, such as observing modes, data transmission system, and correlator setups, are expected to change significantly at the beginning of 2010.**

The basic data produced by the VLA are the visibilities, or measures of the spatial coherence function, formed by correlation of signals from the array’s elements. The most common mode of operation uses these data, suitably calibrated, to form images of the radio sky as a function of sky position and frequency. Another mode of observing (commonly called *phased array*) allows operation of the array as a single element through coherent summation of the individual antenna signals. This mode is commonly used for VLBI observing and for observations of rapidly varying objects, such as pulsars.

The VLA can vary its resolution over a range exceeding a factor of ~ 50 through movement of its component antennas. There are four basic arrangements, called configurations, whose scales vary by the ratios 1 : 3.2 : 10 : 32 from smallest to largest. These configurations are denoted **D**, **C**, **B**, and **A** respectively. In addition, there are 3 ‘hybrid’ configurations labelled **DnC**, **CnB**, and **BnA**, in which the North arm antennas are deployed in the next larger configuration than the SE and SW arm antennas. These hybrid configurations are especially well suited for observations of sources south of $\delta = -15^\circ$ or north of $\delta = +75^\circ$.

Beginning in 1998, the standard **C** configuration was replaced by a slightly modified one, formerly known as **CS**, in which one antenna from the middle of the north arm (N10) is placed at N1 (at the center of the array) to give better short-spacing baseline coverage. See VLA Scientific Memos # 172 and 175, available from Reference 12 (see Section 6).

Traditionally, the VLA has completed one cycle through all four configurations in approximately a 16 month period. However, this cycle will change in early 2010 to accommodate commissioning of the EVLA correlator and the onset of shared-risk science with the EVLA. The present best estimate for the VLA configuration schedule in 2009 and 2010 is presented in Table 3, but prospective users should consult the web page <http://www.vla.nrao.edu/genpub/configs/> or recent NRAO and AAS newsletters for up-to-date schedules and associated proposal deadlines. Refer to Section 4.1 for information on how to submit an observing proposal.

Observing projects on the VLA vary in duration from as short as 1/2 hour to as long as several weeks. Most observing runs have durations of a few to 24 hours, with only one, or perhaps a few, target sources. However, since the VLA is a two-dimensional array, images can be made with data durations of less than one minute. This mode, commonly called *snapshot* mode, is well suited to surveys of relatively strong, isolated objects. See Section

Table 3: Predicted VLA Configuration Schedule for 2009–2010

	Feb–May	Jun–Sep	Oct–Jan
2009	B	C	D_{VLA}
2010	D_{EVLA}	C_{EVLA}	B_{EVLA}

Note: The current plan is to switch over to the new EVLA correlator near the beginning of 2010, with an initially restricted set of modes that includes those necessary to emulate the previous capabilities of the VLA correlator. At that time, the order of configurations is scheduled to be reversed from $A \rightarrow B \rightarrow C \rightarrow D$ to $D \rightarrow C \rightarrow B \rightarrow A$ in order to facilitate commissioning of the new correlator with gradually increasing data rates. This correlator changeover is denoted in the table by the change in configurations from **D_{VLA}** to **D_{EVLA}**.

3.17 for details.

The VLA can be broken into as many as five sub-arrays, each of which can observe a different object at a different band. This is especially useful for multi-band flux density monitoring observations, and for observing compact objects for which the VLA’s full imaging capability and sensitivity are not required. However, important restrictions apply when multiple sub-arrays are used – refer to Section 3.9 for these restrictions.

All VLA antennas are permanently outfitted with receivers for seven wavelength bands centered near $\lambda\lambda$ 90, 20, 6, 3.6, 2.0, 1.3, and 0.7 cm. These bands are commonly referred to as P, L, C, X, U, K and Q bands, respectively. However, the staging of the EVLA antenna retrofits is such that the EVLA antennas have the old 2-cm systems removed, and they will not be replaced with new wideband systems until 2010 and later. Thus, the maximum number of antennas with 2 cm available has decreased to only a few antennas in 2009; at present, this generally is not a useful observing band for observers. Furthermore, a technical problem with the P band system has been encountered and P band observations are not currently recommended. However, a new receiving system centered near λ 1.0 cm (33 GHz, ‘Ka-band’) is beginning to be implemented on EVLA antennas, and a special call for first observing with this band is being made in January 2009. See Section 3.3 for more details about the availability of new bands and enhanced frequency tunability for EVLA antennas.

The 74 MHz system (also known as the ‘4-band’ system) is now available on all antennas, but is not permanently installed. The long dipoles needed to efficiently illuminate the antennas have been shown to reduce the gain and increase the system temperature at 20 cm by about 5%. Because of this, and the experimental nature of this frequency band, we will continue past practice of mounting the dipoles for limited periods of time during which 74 MHz observing is concentrated. At present, this means that, provided a sufficient number of project hours at 74 MHz have been approved, dipoles are mounted near the end of the **A** configuration for observations in the **A**, **BnA** and **B** configurations. Typically, there has not been sufficient proposal pressure to mount the dipoles in the more compact VLA configurations, although a special observing session for **CnB** and **C** configurations was carried out in late 2006.

The VLA antennas in the array can tune to two different frequencies from the same wavelength band provided the frequency difference does not exceed approximately 450 MHz (the EVLA antennas can have frequencies separated by considerably more; see Section 3.3). Right-hand circular (RCP) and left-hand circular (LCP) polarizations are received for both frequencies. Each of these four data streams is called an ‘IF’ (for ‘Intermediate Frequency’ channel). These four data streams are known in VLA-ese as IFs ‘A’, ‘B’, ‘C’, and ‘D’. IFs A and B receive RCP, IFs C and D receive LCP. IFs A and C are always at the same

frequency, as are IFs B and D. [But the (A,C) frequency is usually different from the (B,D) frequency.] The array also can observe simultaneously one frequency within L band and one within P band (known as LP), or one within 4-band and one within P band (known as 4P mode). However, the P band receivers have been found to be incompatible with the wideband EVLA electronics due to strong, internally-generated interference. P band observations are not recommended until this problem has been solved.

Observations at seven different bandwidths (given by $50/2^n$ MHz, with $n = 0, 1, \dots, 6$) are possible¹. A 200 kHz bandwidth is also available in spectral line mode, but suffers seriously from aliasing on EVLA antennas due to the hardware used to feed the digital EVLA signals into the VLA correlator. Observations using 200 kHz bandwidth are not currently recommended, and users considering using this bandwidth should first consult VLA staff. Different bandwidths can be used for each of the two separate frequencies. Wider bandwidths provide better sensitivity, but also increase the chromatic aberration. Refer to Section 3.5.2 for details.

The VLA correlator has two basic modes, *Continuum* and *Spectral Line*. In *Continuum mode*, the correlator provides the four correlations (RR, RL, LR, LL) needed for full polarimetric imaging at both frequencies. This mode is particularly well suited to high sensitivity, narrow field-of-view projects. The *Spectral Line mode* is a spectrum-measuring mode principally intended for observing spectral lines. There are many options allowed in this mode. Besides its use for all spectral line projects, certain continuum projects which require extremely high dynamic range, or large field-of-view at high spatial resolution, will benefit from use of this mode. (These are sometimes referred to as *multichannel continuum* or *pseudo-continuum* projects.) This mode also is used to great advantage when RFI (Radio Frequency Interference) is expected within the bandpass. The Spectral Line modes are further described in Section 3.15.

3 PERFORMANCE OF THE VLA

This section contains details of the VLA's resolution, sensitivity, tuning range, dynamic range, pointing accuracy, and modes of operation. Detailed discussions of most of the observing limitations are found elsewhere. In particular, see References 1 and 2, listed in Section 6.

3.1 Resolution

The VLA's resolution is generally diffraction-limited, and thus is set by the array configuration and frequency of observation. It is important to be aware that a synthesis array is 'blind' to structures on angular scales both smaller and larger than the range of fringe spacings given by the antenna distribution. For the former limitation, the VLA acts like any single antenna – structures smaller than the diffraction limit ($\theta \sim \lambda/D$) are broadened to the resolution of the antenna. The latter limitation is unique to interferometers – it means that structures on angular scales significantly larger than the fringe spacing formed by the shortest baseline are not measured. No subsequent processing can fully recover this missing information, which can only be obtained by observing in a smaller array configuration,

¹The VLA's maximum bandwidth is commonly referred to as 50 MHz per IF, but the actual effective bandwidth is closer to 43 MHz, due to bandpass roll-off.

using the mosaicing method, or with an instrument (such as a large single antenna) which provides this information.

Table 4 summarizes the relevant information. This table shows the maximum and minimum antenna separations, the approximate synthesized beam size (full width at half-power), and the scale at which severe attenuation of large scale structure occurs.

A project with the goal of doubling the longest baseline available in the **A** configuration by establishing a real-time fiber optic link between the VLA and the VLBA antenna at Pie Town was carried out in the late 1990s, and used operationally through 2005. This link is no longer operational; there is a goal (unfunded, at present) of implementing a new digital Pie Town link after the EVLA is operational.

3.2 Sensitivity

Table 5 shows the VLA sensitivities expected for natural weighting of the visibility data. The values listed are the expected rms fluctuations due to thermal noise on an image, calculated using the standard formulae with the system temperatures and efficiencies listed. A maximum number of 25 antennas is used in these calculations (except for U band); at any given time, it is assumed that 3 of the possible 28 antennas are missing, one each for EVLA mechanical retrofitting, EVLA electronics outfitting, and EVLA commissioning. Hardware limitations prevent us from inputting more than 22 EVLA antennas to the old VLA correlator, and no more than 25 antennas will be available by the end of 2009. The tabulated sensitivity values are realized in practice except at low frequencies and in smaller configurations where the sensitivities are limited by confusing sidelobes from objects outside the image. The rms limit due to confusing sources for the VLA in **D** configuration is estimated in Table 5. Another case where the thermal rms noise will not be achieved is in imaging very bright objects where the residual image noise is due to baseline dependent errors (‘closure errors’ – see 3.11).

For a comparison, Table 6 gives the sensitivity goals of the EVLA, including the expectations based on achieved values for those receivers that already have been implemented.

In general, the expected point-source rms noise in mJy on an output image, for natural weighting, can be calculated with the following formula:

$$\Delta I_m = \frac{K}{\sqrt{N(N-1)(N_{\text{IF}}T_{\text{int}}\Delta\nu_{\text{M}})}} \text{ mJy} \quad (1)$$

where N is the number of antennas, T_{int} is the total on-source integration time in hours, $\Delta\nu_{\text{M}}$ is the effective continuum bandwidth or spectral-line channel width in MHz, and N_{IF} is the number of IFs (from 1 to 4) or spectral line channels (from 1 to 512) which will be combined in the output image². K is a system constant, equal to 1000, 50, 8.0, 7.8, 6.6, 27, 14, and 35³ for 4, P, L, C, X, U, K, and Q bands respectively. This constant K also can be expressed in terms of system temperature and efficiency as:

$$K = \frac{0.12T_{\text{sys}}}{\eta_a} \quad (2)$$

²For most continuum observations, N_{IF} will be either 4 (all IFs), or 2 (one IF pair), and $\Delta\nu_{\text{M}}$ will be the IF bandwidth. Thus, $N_{\text{IF}} = 2$ for Stokes’ Q, U and (true) I images at a single frequency. For spectral line work, $\Delta\nu_{\text{M}}$ is the spectral resolution (channel width) in MHz.

³The quoted value of K for Q-band assumes a dry and stable atmosphere, and excellent pointing characteristics.

Table 4: Configuration Properties

Configuration	A	B	C	D
B_{\max} (km ⁽¹⁾)	36.4	11.4	3.4	1.03
B_{\min} (km ⁽¹⁾)	0.68	0.21	0.035 ⁽⁵⁾	0.035
	Synthesized Beamwidth θ_{HPBW} (arcsec) ^(1,2,3)			
400 cm	24.0	80.0	260.0	850.0
90 cm ⁽⁶⁾
20 cm	1.4	3.9	12.5	44.0
6 cm	0.4	1.2	3.9	14.0
3.6 cm	0.24	0.7	2.3	8.4
2 cm ⁽⁶⁾
1.3 cm	0.08	0.3	0.9	2.8
1.0 cm ⁽⁶⁾
0.7 cm	0.05	0.15	0.47	1.5
	Largest Angular Scale θ_{LAS} (arcsec) ^(1,4)			
400 cm	800.0	2200.0	20000.0	20000.0
90 cm ⁽⁶⁾
20 cm	38.0	120.0	900.0	900.0
6 cm	10.0	36.0	300.0	300.0
3.6 cm	7.0	20.0	180.0	180.0
2 cm ⁽⁶⁾
1.3 cm	2.0	7.0	60.0	60.0
1.0 cm ⁽⁶⁾
0.7 cm	1.3	4.3	43.0	43.0

These estimates of the synthesized beamwidth are for a uniformly weighted, untapered map produced from a full 12 hour synthesis observation of a source which passes near the zenith.

Footnotes:

1. B_{\max} is the maximum antenna separation, B_{\min} is the minimum antenna separation, θ_{HPBW} is the synthesized beam width (FWHM), and θ_{LAS} is the largest scale structure ‘visible’ to the array.
2. The listed resolutions are appropriate for sources with declinations between -15 and 75 degrees. For sources outside this range, the extended north arm hybrid configurations (**BnA**, **CnB**, **DnC**) should be used, and will provide resolutions similar to the smaller configuration of the hybrid, except for declinations south of -30 . No double-extended north arm hybrid configuration (e.g., **CnA**, or **DnB**) is provided.
3. The approximate resolution for a naturally weighted map is about 1.5 times the numbers listed for θ_{HPBW} . The values for snapshots are about 1.3 times the listed values.
4. The largest angular scale structure is that which can be imaged reasonably well in full synthesis observations. For single snapshot observations the quoted numbers should be divided by two.
5. The standard **C** configuration has been replaced by a slightly modified one, formerly known as **CS**, wherein an antenna from the middle of the north arm has been moved to the central pad ‘N1’. This results in improved imaging for extended objects, but will degrade snapshot performance. Although the minimum spacing is the same as in **D** configuration, the surface brightness sensitivity to extended structure is considerably inferior to that of the **D** configuration (but considerably better than standard **C** configuration).
6. Data on resolution and largest angular size are not included for the 90 cm band because of the technical issues with this band mentioned in Section 2. Neither of the 2 cm and 1.0 cm bands has a full complement of antennas, so the exact values depend on the rate of antenna outfitting and the placement of individual antennas in the various configurations. As the number of antennas equipped at 1.0 cm increases, the relevant angular scales will approach values roughly mid-way between those at 0.7 cm and those at 1.3 cm.

Table 5: VLA Sensitivity in Mid-2009

Frequency (GHz)	Band Name		System Temperature ⁽¹⁾ (K)	Antenna Efficiency ⁽²⁾ (%)	Number Antennas (VLA+EVLA)	RMS (10 min) Sensitivity (mJy)
	Approximate Wavelength	Letter Code				
0.073 - 0.0745	400 cm	4	1000-10000	15	5+20	160 ⁽³⁾
0.3 - 0.34	90 cm	P	150-180	40	≤ 10	> 4 ⁽³⁾
1.24 - 1.70	20 cm	L	35	55	5+20	0.061
4.5 - 5.0	6 cm	C	45	69	5+20	0.058
8.1 - 8.8	3.6 cm	X	35	63	5+20	0.049
14.6 - 15.3	2 cm	U	120	58	5+0	1.0
22.0 - 24.0	1.3 cm	K	50 - 80	40	5+20	0.11 ⁽⁴⁾
40.0 - 50.0	0.7 cm	Q	80	35	5+20	0.27 ⁽⁵⁾

Frequency (GHz)	Wavelength	RMS Point-Source Sensitivity (12 hours) (mJy)	Beam-averaged Brightness Sensitivity ⁽⁶⁾ (D-config) (mKelvins)	Antenna Primary Beam Size (FWHP) θ_{PB}	Peak/Total Confusing Source in Beam (Jy)	RMS Confusion Level (D-config) (μ Jy/beam)
0.073 - 0.0745	400 cm	17 ⁽³⁾	2000	700'	20/350	lots
0.3 - 0.34	90 cm	0.18 ⁽³⁾	21.3	150'	1.8/15	4400
1.24 - 1.70	20 cm	0.0071	0.8	30'	0.11/0.35	86
4.5 - 5.0	6 cm	0.0069	0.8	9'	0.002	3.6
8.1 - 8.8	3.6 cm	0.0057	0.6	5.4'	0.001	0.89
14.6 - 15.3	2 cm
22.0 - 24.0	1.3 cm	0.013 ⁽⁴⁾	1.5	2'	0.00001	—
40.0 - 50.0	0.7 cm	0.032 ⁽⁵⁾	3.8	1'	—	—

All sensitivity calculations assume 43 MHz bandwidth per IF, (except for P-band and 4-band, where 3.125 MHz and 0.78 MHz are used), two IF pairs (four IFs), natural weighting, and an elevation of 45 degrees. Five VLA and 20 EVLA antennas are assumed, as will be the case in the period near the middle of 2009; since there will be only a few VLA antennas remaining with 2 cm installed, most information regarding this band has been removed. EVLA antennas are assumed to have the same performance as VLA antennas, although they will be significantly better at some bands (particularly at 6 cm = C band); since we mostly have “transition” EVLA receivers at present, the final system temperatures are not yet available. Performance will degrade for large zenith angles at high frequencies and for sources close to the galactic plane at low frequencies. The confusion limits (see Condon 2002, ASP Conf. 278, p. 155) for C configuration are approximately a factor of 10 less than those tabulated above for D configuration.

Footnotes:

1. Temperature ranges listed at P, K, and Q bands include sky temperature variations due to the galactic plane (P-band) or Earth’s atmosphere (K band). System temperatures for VLA antennas at L band are increased substantially at elevations below 45° due to ground pickup; this effect is considerably reduced (though not completely eliminated) in the EVLA antennas because of their larger L band feeds.
2. This is the system efficiency without the correlator factor (about 0.78). Efficiencies at U, K, and Q bands at low elevations (< 30 degrees) are considerably decreased due to gravitational distortions of the antenna figure.
3. Value listed for 74 MHz assumes observations near the galactic poles, and ‘3-D’ imaging. Snapshot observations will not usually reach this level, as the confusion problem is insoluble with only snapshot u,v coverage. Full-beam A configuration deconvolution at 74 MHz will be calibration-limited due to the non-isoplanatic ionosphere. At 327 MHz the imaging will be very poor due to the limited number of receivers available with this sensitivity.
4. Listed sensitivity is for El = 45° and very dry atmosphere at 22 GHz. A wet atmosphere can increase zenith opacity from 5 to 15 percent, and increase the sky temperature from 10 to 40 K.
5. Listed sensitivity is for El = 45° and dry atmosphere at 43 GHz. A wet atmosphere can increase zenith opacity from 6 to 8 percent, and increase the zenith sky temperature from 15 to 24 K. Atmospheric attenuation and temperature increase dramatically with increasing frequency – sky temperatures exceeding 55 K and zenith opacity of 25 percent are expected at 49 GHz.
6. Values listed assume a uniform source that fills the synthesized beam in D configuration. Since natural weighting is assumed, the beam sizes are ~50% larger in each dimension than the values given in Table 4.

Table 6: **EVLA Sensitivity Goals**

Band ⁽¹⁾ (GHz)	Band Code	S_E ⁽²⁾ req. (Jy)	S_E ⁽²⁾ actual (Jy)	Cont. Sens. 1σ , 9 hr (μ Jy)	Line Sens. 1σ , 1 km s ⁻¹ , 9 hr (mJy)
1 - 2	L	325	335	1.6	0.5
2 - 4	S	235	TBD	TBD	TBD
4 - 8	C	245	250	0.5	0.2
8 - 12	X	300	TBD	TBD	TBD
12 - 18	Ku	385	TBD	TBD	TBD
18 - 26.5	K	650	450	0.6	0.2
26.5 - 40	Ka	760	675	0.85	0.2
40 - 50	Q	1200	1400 ⁽³⁾	1.8	0.4

Footnotes:

1. Performance parameters in the bands above 18 GHz are based on actual performance for the final receiver designs. Performance parameters for the 1–2 and 4–8 GHz bands are for interim systems; the final systems are expected to be slightly better. The remaining three bands are presently in the design and prototyping stages.
2. The parameter S_E is the ‘‘System Equivalent Flux Density’’, a measure of the flux density of a natural radio source that would be required to double the system temperature. Thus, lower values of S_E are better. S_E is given by the equation $S_E = 5.62T_{\text{sys}}/\epsilon$, where T_{sys} is the total system temperature of the receiver and ϵ is the antenna aperture efficiency in the given band. Two values of S_E are given, first the required value from the EVLA Project Book, followed by the actual achieved value.
3. The final performance of the 40–50 GHz systems is expected to be somewhat better than tabulated. Because the EVLA feed is at a different feed-circle location than the previous VLA feed, a new round of holography measurements and re-setting of antenna panels will still be necessary to optimize performance at the highest frequency band. There is some expectation for minor improvement in the 26.5–40 GHz band as well after panel re-setting.

where T_{sys} is the system temperature, and η_a is the antenna efficiency, as listed in Table 5. (A correlator efficiency of 0.78 has already been incorporated into this expression). For the more commonly used uniform weighting employing the robust weight scheme intermediate between pure natural and pure uniform weightings (available in the AIPS task **IMAGR**), the sensitivity will be a factor of about 1.2 worse than the listed values. To aid VLA proposers there is an exposure tool calculator on-line at <http://www.vla.nrao.edu/astro/guides/exposure/> that provides a graphical user interface to these equations.

It is important to note that these listed sensitivities are calculated from data taken in optimum conditions. For many bands, the system temperature and gain are significant functions of elevation and weather conditions (see next section).

A useful alternate form of the point-source sensitivity equation is

$$\Delta I_m = \frac{42.4K}{\sqrt{N_{\text{pts}}N_{\text{IF}}\Delta t_{\text{int}}\Delta\nu_M}} \text{ mJy} \quad (3)$$

where N_{pts} is the number of visibility points (which is listed in the AIPS header), and Δt_{int} is the integration time per visibility in seconds. N_{IF} , $\Delta\nu_M$ and K are defined as above.

The beam-averaged brightness temperature measured by a given array depends on the

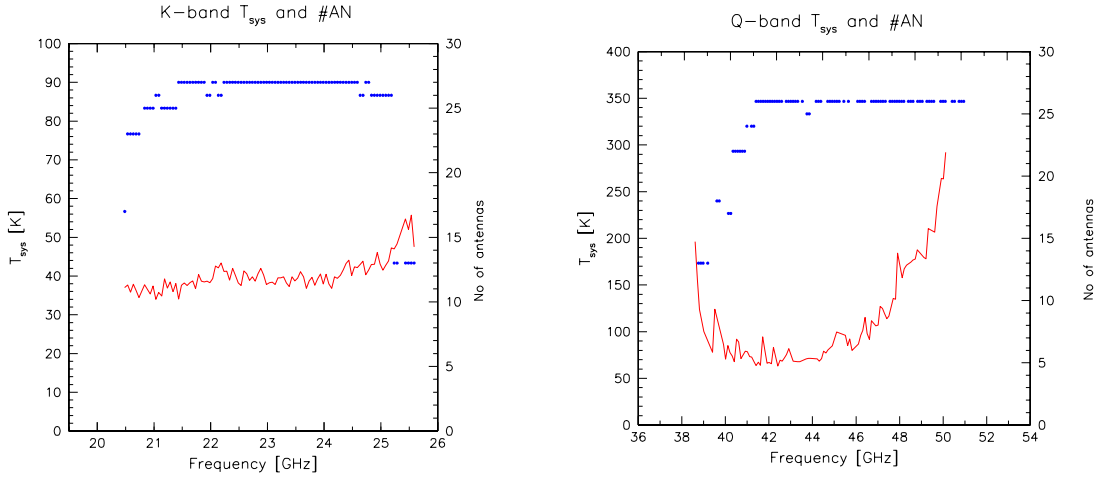


Figure 1: **System Temperatures vs. Frequency at K and Q bands.** Above are plots of the system temperature (solid red line) versus observing frequency at K and Q bands. The data were taken during night time in May 2003, under very good weather conditions. This plot shows that the system temperature is stable across the band. In blue is the number of antennas that successfully locked at the given frequency.

synthesized beam, and is related to the flux density by

$$T_b = \frac{S\lambda^2}{2k\Omega} = F \cdot S \quad (4)$$

where T_b is the brightness temperature (Kelvins) and Ω is the beam solid angle. For natural weighting (where the angular size of the approximately Gaussian beam is $\sim 1.5\lambda/B_{\max}$), and S in mJy per beam, the constant F depends only upon array configuration and has the approximate value $F = 190, 19, 1.6, 0.15$ for **A**, **B**, **C**, and **D** configurations, respectively. The brightness temperature sensitivity can be obtained by substituting the rms noise, ΔI_m , for S . Note that Equation 4 is a *beam-averaged* surface brightness; if a source size can be measured the source size and integrated flux density should be used in Equation 4, and the appropriate value of F calculated. A more detailed description of the relation between flux density and surface brightness is given in Chapter 7 of Reference 1, listed in Section 6.

For observers interested in HI in galaxies, a number of interest is the sensitivity of the observation to the HI mass. This is given by van Gorkom et al. (1986; AJ, 91, 791):

$$M_{\text{HI}} = 2.36 \times 10^5 D^2 \sum S\Delta V M_{\odot} \quad (5)$$

where D is the distance to the galaxy in Mpc, and $S\Delta V$ is the HI line area in units of Jy km/s.

The sensitivity varies across each observing band. Table 7 gives the frequency ranges for each band at which the sensitivity degrades by 10% and by a factor of two for the VLA receivers. Also included are the maximum ranges over which the VLA receivers remain operative. At these extreme ends, the system sensitivity is typically 10 to 100 times worse

Table 7: Sensitivity Ranges of VLA Bands

Band	0.9 x Nominal	0.5 x Nominal	Extreme Range
90 cm	305 - 337 MHz	303 - 342 MHz	298 - 345 MHz
20 cm	1240 - 1700 MHz	1170 - 1740 MHz	1150 - 1750 MHz
6 cm	4500 - 5000 MHz	4250 - 5100 MHz	4200 - 5100 MHz
3.6 cm	8080 - 8750 MHz	7550 - 9050 MHz	6800 - 9600 MHz
2 cm	14650 - 15325 MHz	14250 - 15700 MHz	13500 - 16300 MHz
1.3 cm	21200 - 25200 MHz	20600 - 25200 MHz	20400 - 25500 MHz
0.7 cm	40500 - 44500 MHz	39000 - 47500 MHz	38000 - 51000 MHz

than at band center. Furthermore, not all antennas will operate at these frequencies. For similar information for EVLA antennas, see Section 3.3. In Figure 1, we show the system temperature and number of operable antennas plotted as a function for frequency for K and Q bands.⁴ For all bands, consider consulting a VLA staff scientist if you wish to observe near the band edges.

In view of the importance of observations at the lower edge of the 20-cm band for studies of red-shifted HI, some special words are appropriate to describe the performance of the VLA receivers at frequencies below 1250 MHz. The roll-off of this band at the low frequency edge is very gentle, and useful observations at 1155 MHz and lower have been made. However, not all frequencies can be tuned, as tests have shown there are four 10 MHz wide ‘notches’, centered at 1212, 1182, 1162 and 1150 MHz, within which the array can take no useful data. These notches exist in both RR and LL correlations but vary in shape and central frequency from antenna to antenna. A plot of the relative sensitivity between 1150 and 1250 MHz for the VLA receivers is shown in Figure 2.

The sensitivity at the low frequency bands (90 cm and 400 cm) is difficult to parameterize. There are two important effects which limit the sensitivity.

1. The diffuse galactic background contributes an important fraction of the total system temperature – especially at 400 cm, where it is the only important contributor. This means that the sensitivity will vary by nearly a factor of 10 between locations on the galactic plane and locations near the galactic poles.
2. The primary beam at both bands is very broad, and the sidelobe levels comparatively high, resulting in significant sensitivity to objects far from the target object. Because of the difficulty in imaging very large fields of view (due to the non-coplanar baseline effect, see Section 3.5.4, and the non-isoplanicity over large angles), the sidelobes of undeconvolved objects in non-imaged areas (essentially the entire 2π steradians visible to the antennas!) will appear in the map of the target source. Use of the AIPS program IMAGR will permit removal of the major background objects, and should result in a sensitivity not worse than a factor of two higher than that expected on the basis of the system temperature.

⁴The number of operable antennas was determined when all antennas had old VLA electronics; the retrofitted EVLA antennas have wider tuning capabilities.

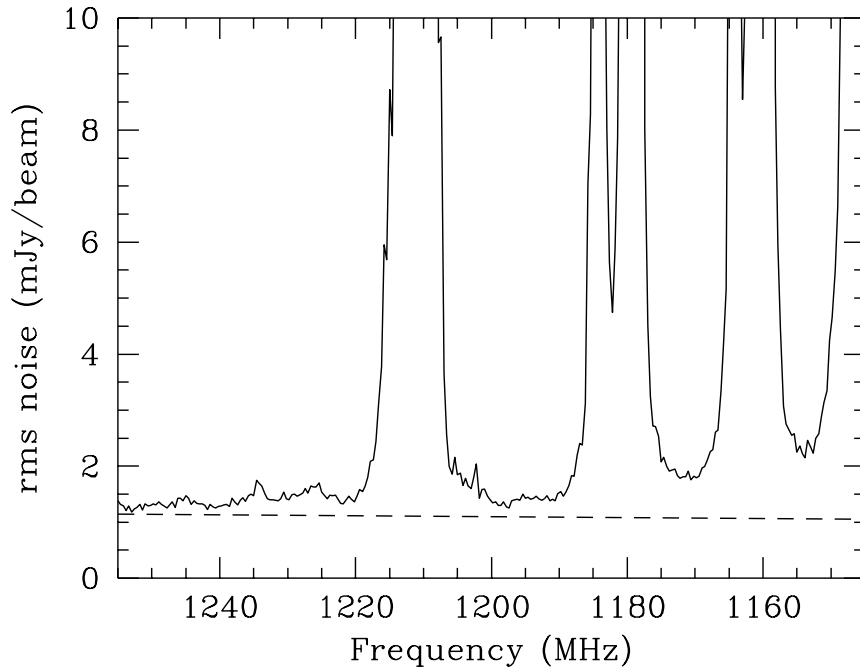


Figure 2: **VLA Sensitivity Between 1150 and 1250 MHz.** This plot shows the relative sensitivity of the VLA at the lower end of the 20 cm band. The dashed line represents the sensitivity at the center of the band, so it can be seen that serious degradation in sensitivity is not notable until below 1190 MHz. The four ‘notches’ are instrumental in origin.

3.3 EVLA Frequency Bands and Tunability

The EVLA electronics and local-oscillator systems enable tuning over wider frequencies, which is possible with the wideband feeds being installed on retrofitted antennas (or already present at K and Q bands). At this writing, wider-band tuning capabilities are available at L, C, K, and Q bands (mostly with interim EVLA receivers at L and C bands), and the new 1.0 cm band will be available on at least 14 antennas in mid-2009. For example, the new C band tuning enables observations of methanol at 6.7 GHz, while the new K band tuning enables observations of the 22.235 GHz H₂O line at redshifts up to $z \approx 0.18$. Figure 3 shows the present plan for EVLA receiver deployment over the remainder of the EVLA Construction Project, while Table 8 gives a prediction of the new frequency capabilities that we expect in June 2009 and December 2009.

Figure 3 does not tell the entire story of frequency availability for observing with the VLA, since there also are some interim receivers that may be used in the absence of the final EVLA receivers. Thus Figures 4 and 5 give more detailed schedules for each frequency band, including the presence of these interim receivers.

The new Ka-band system is most sensitive around 33 GHz, and the default continuum frequency has been set to 33.5 GHz. The K factor to be used in calculating expected sensitivities at the default continuum frequency is 20. The relative sensitivity as a function of frequency across the entire band is shown in Figure 6.

IFs B and D are able to tune over the full 26.5 to 40 GHz, while IFs A and C cover 32–40 GHz. IFs B/D must also be tuned to a lower frequency than IFs A/C. For the EVLA

EVLA Wideband Receiver Availability

Prepared Dec 2008

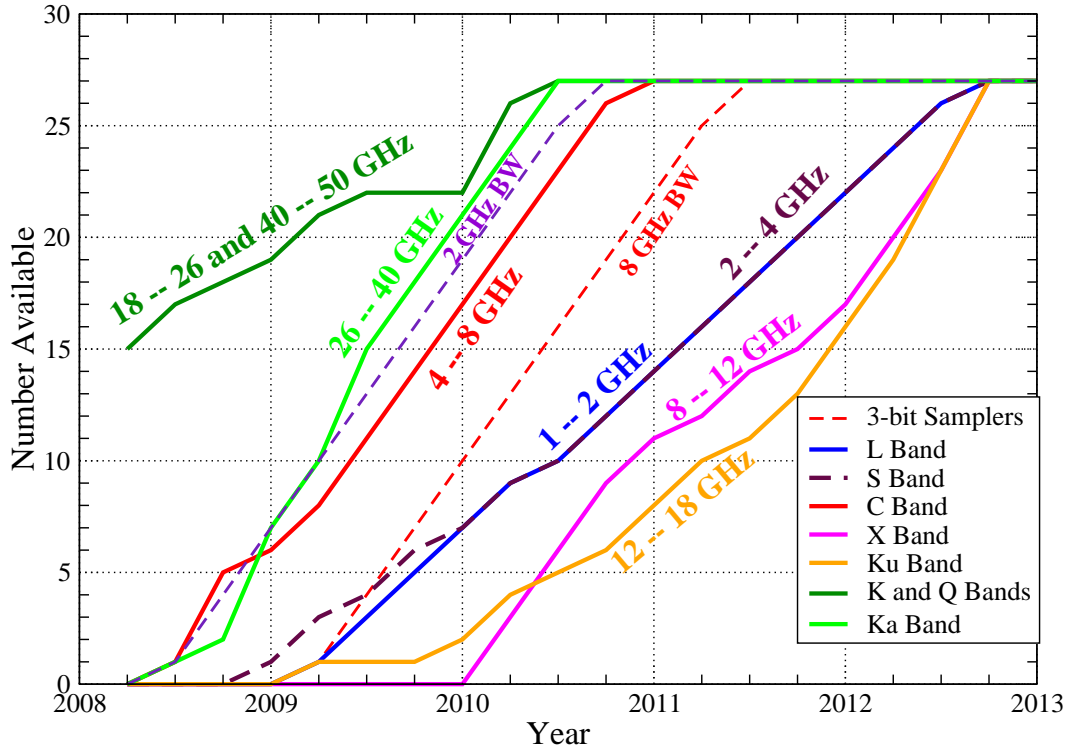


Figure 3: **EVLA Receiver Deployment Plan.** Above is a plot of the availability of the final EVLA receivers from 2008 until the end of the EVLA Construction Project in 2012. Only final EVLA receivers are shown. Interim receivers with reduced frequency coverage or polarization purity are available at some bands, and are shown in other figures. Approximate installation dates for 2-GHz and 8-GHz bandwidths per polarization also are shown, but these will not be accessible to observers until after the transition from the VLA correlator to the EVLA (WIDAR) correlator and the full commissioning of the new correlator.

Ka-band receivers it is possible to tune the two IF pairs up to 11 GHz apart, while for other EVLA receivers the IFs can be separated by the full tuning range. Please check with VLA staff before attempting observations outside the standard VLA tunings.

3.4 Elevation Effects

The VLA’s antenna performance changes with elevation. These changes are significant at L, U, K, and Q bands, and must be corrected for high-precision imaging.

The loss of performance is due to two different effects:

1. The sky and ground temperature contributions to the total system temperature increase with decreasing elevation. This effect is very strong at L, K, and Q bands, as shown in Figure 7, and is relatively unimportant at the other bands. The source of the excess noise at L-band is the ground itself (‘spillover’), due to the microwave lens feed structure; this effect is greatly reduced in retrofitted EVLA antennas, as shown

Table 8: **Tuning Ranges of EVLA Bands**

Band	Range	Final EVLA Receivers Available	
		June 2009	December 2009
20 cm (L)	1.2 - 2.0 GHz	3	7
13 cm (S)	2.0 - 4.0 GHz	4	7
6 cm (C)	4.0 - 8.0 GHz	11	17
3 cm (X)	8.0 - 12.0 GHz	0	0
2 cm (U)	12.0 - 18.0 GHz	1	2
1.3 cm (K)	18.0 - 26.5 GHz	22	22
1 cm (Ka)	26.5 - 40.0 GHz	15	21
0.7 cm (Q)	40.0 - 50.0 GHz	22	22

Note: The rightmost columns give the numbers of final EVLA receivers available at each band; additional interim receivers with poorer polarization purity are available in the 1–2 GHz and 4–8 GHz bands, while the old narrow-band VLA receivers are still available in the 8–8.8 GHz band.

Evolution of Receiver Capability on the EVLA

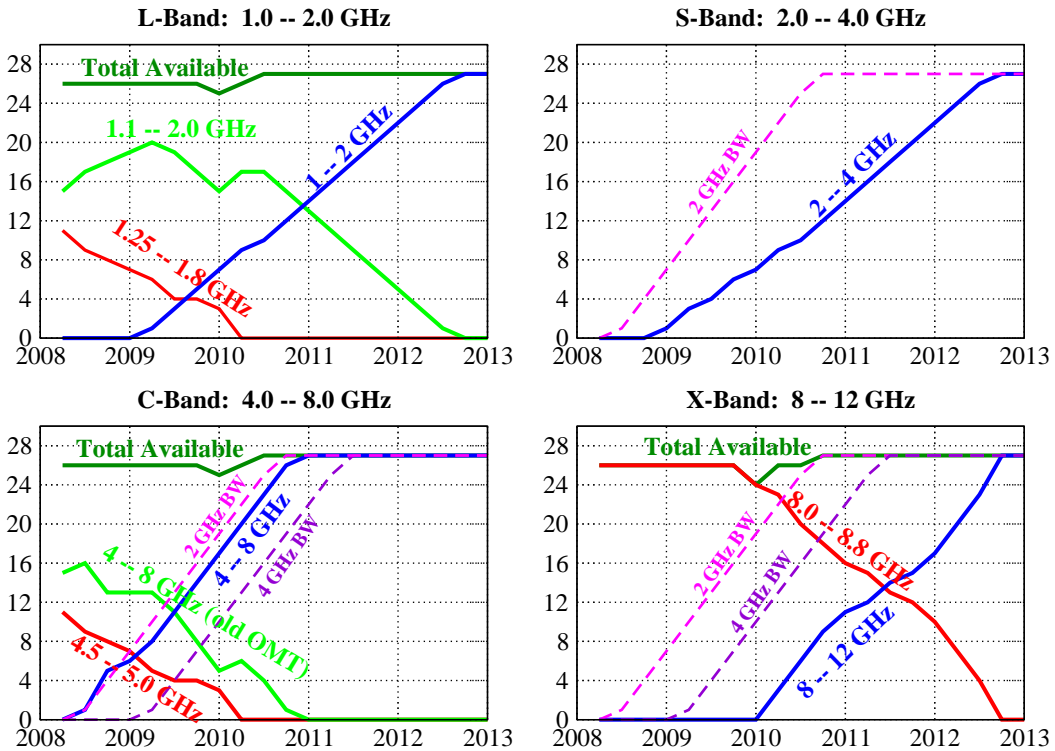


Figure 4: **Low-frequency Receiver Availability.** Above is a plot of the receiver availability at the four lowest-frequency EVLA bands, between 1 and 12 GHz, from 2008 through the end of 2012. For each plot, the red line shows the number of old VLA receivers available, the light green line shows the availability of interim EVLA receivers (typically with increased bandwidth coverage but without optimal polarization performance), and the blue line shows the availability of final EVLA receivers.

Evolution of Receiver Capability on the EVLA

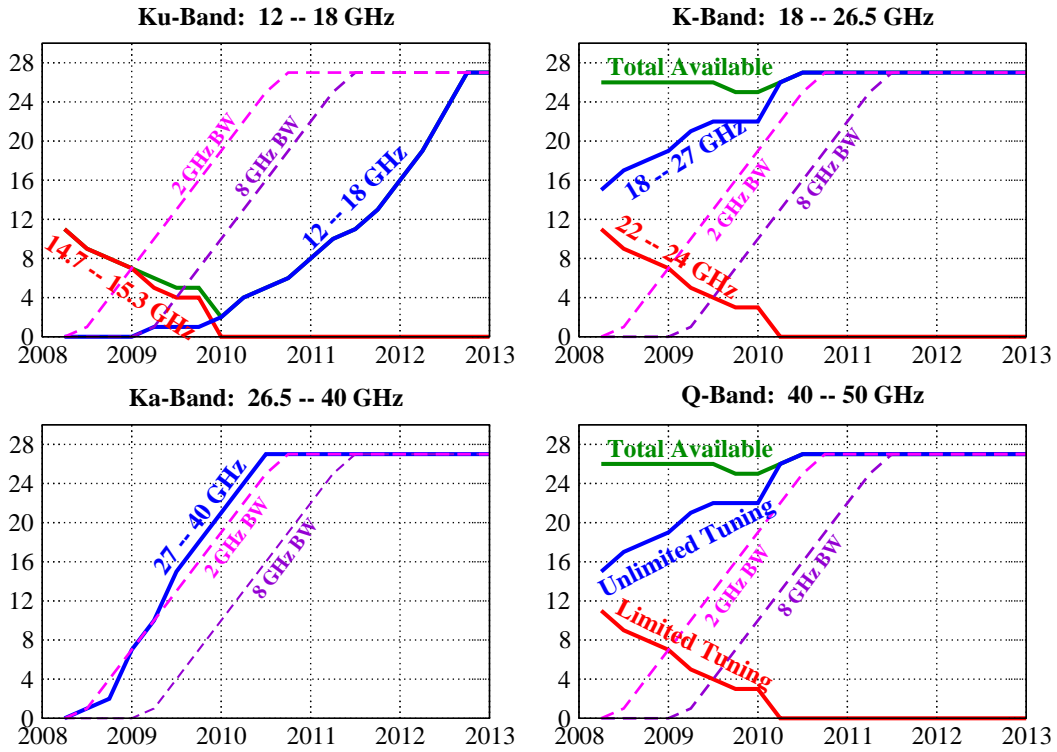


Figure 5: **High-frequency Receiver Availability.** Above is a plot of the receiver availability at the four highest-frequency EVLA bands, between 12 and 50 GHz, from 2008 through the end of 2012. For each plot, the red line shows the number of old VLA receivers available, typically with more limited tuning capability, and the blue line shows the availability of final EVLA receivers.

in Figure 8. At K and Q bands, the extra noise comes directly from atmospheric emission, primarily from water vapor at K-band, and from water vapor and the broad wings of the strong 60 GHz O₂ transitions at Q-band.

In general, the zenith atmospheric opacity to microwave radiation is very low – typically less than 0.01 at L and C and X bands, 0.02 at U band, 0.05 to 0.2 at K band, and 0.05 to 0.1 at the lower half of Q band, rising to 0.3 by 49 GHz. The opacity at K band displays strong variations with time of day and season, primarily due to water vapor. Conditions are best at night, and in the winter. Q band opacity, caused by O₂ in the atmosphere, is considerably less variable.

Observers should remember that clouds, especially clouds with large water droplets (read, thunderstorms!), can add appreciable noise to the system temperature. Significant increases in system temperature can, in the worst conditions, be seen at wavelengths as long as 6 cm.

2. The antenna figure degrades at low elevations, leading to diminished forward gain at the shorter wavelengths. In general, the forward power gain of the antennas can be well fitted by a simple parabola of form: $G(E) = G_0 - G_2(E - E_m)^2$, where E is

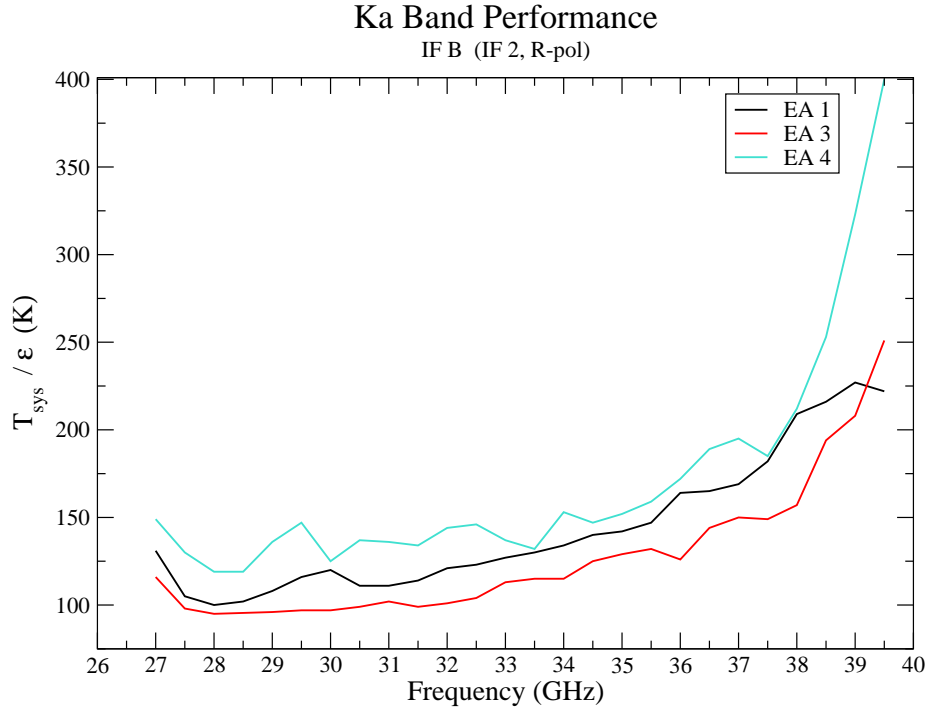


Figure 6: **Ka-band sensitivity as a function of frequency.**

the elevation (in degrees), and E_m is the elevation of maximum forward gain. The average coefficients G_0 , G_2 , and E_m are given in Table 9. The gain-elevation effect is negligible at frequencies below 8 GHz.

Table 9: **Average Power Gain Coefficients for the VLA Antennas**

Band	G_0	G_2	E_m
Q	1.00	3.0×10^{-4}	50
K	1.00	1.5×10^{-4}	58
U	1.00	3.6×10^{-5}	46
X	1.00	0.7×10^{-5}	50

These power coefficients are not directly useful for correcting the effects of antenna gain loss, which require the individual antenna (inverse) voltage correction factors expressed as the coefficients of a polynomial fit to the voltage gain as a function of zenith distance. That is, the AIPS suite of programs can implement gain corrections of the form

$$V_c = G_0 + G_1 Z + G_2 Z^2 + \dots,$$

where V_c is the voltage gain correction of an antenna-IF, and the G_i are the coefficients of a polynomial series. Z is the zenith angle in degrees: $Z = 90 - E$. The preferred method for determining these is through direct measurement of the relative system gain using the AIPS task ELINT on data from a strong calibrator which has been observed over a wide range of elevation.

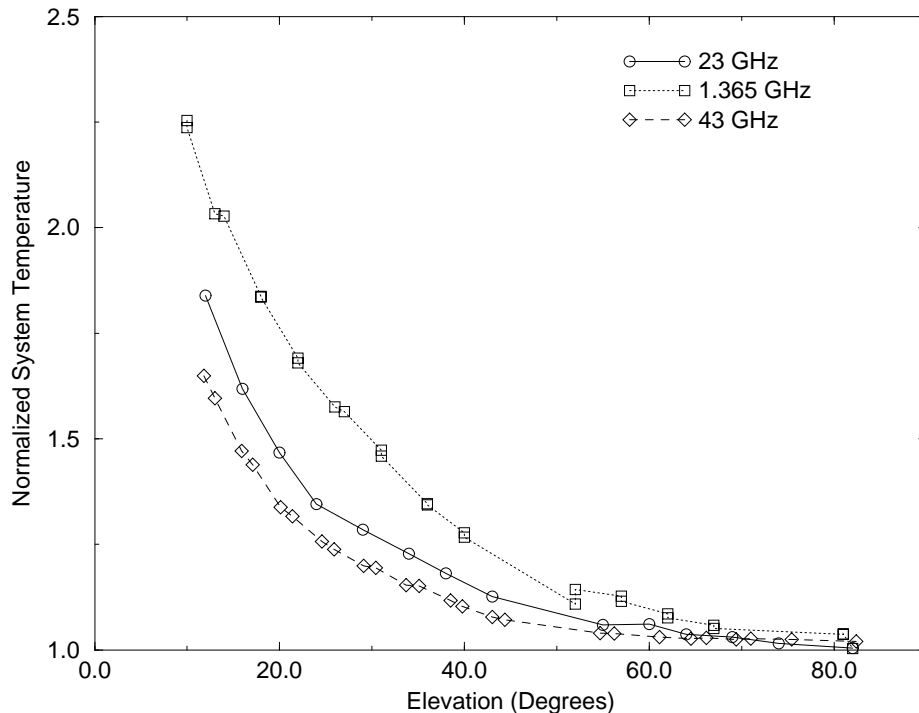


Figure 7: **System Temperature Variations with Elevation at L, K, and Q Bands.** The data have been normalized by the system temperature at the zenith – approximately 80K at 43 GHz, 170K at 23 GHz, and 35K at 1365 MHz. The observations were taken in good weather conditions. Since production of the data for this figure, the VLA 22 GHz receivers were replaced by receivers with much-improved low-noise amplifiers, dramatically reducing the overall system temperature (see Table 5), thus raising the fractional variation at low elevations.

Starting with the 31DEC01 AIPS, the task FILLM applies standard gains and an estimated opacity in CL table version 1. (This correction can be turned off with appropriate parameter choices.) For those with older versions of AIPS or less recent observations, an approximate correction can be obtained using the amplitude coefficients given below in Table 10. These are applied using the AIPS task CLCOR.

Table 10: **Average Inverse Voltage Gain Coefficients for the VLA Antennas**

Band	G_0	G_1	G_2
Q	1.00	-1.29×10^{-2}	1.59×10^{-4}
K	1.00	-0.41×10^{-2}	0.69×10^{-4}
U	1.00	-0.17×10^{-2}	0.19×10^{-4}
X	1.00	-0.23×10^{-3}	0.33×10^{-5}

These coefficients are averages over all the antennas, and are appropriate for an atmosphere of zero opacity. Considerable differences exist among antennas, particularly for antennas #1 and #2.

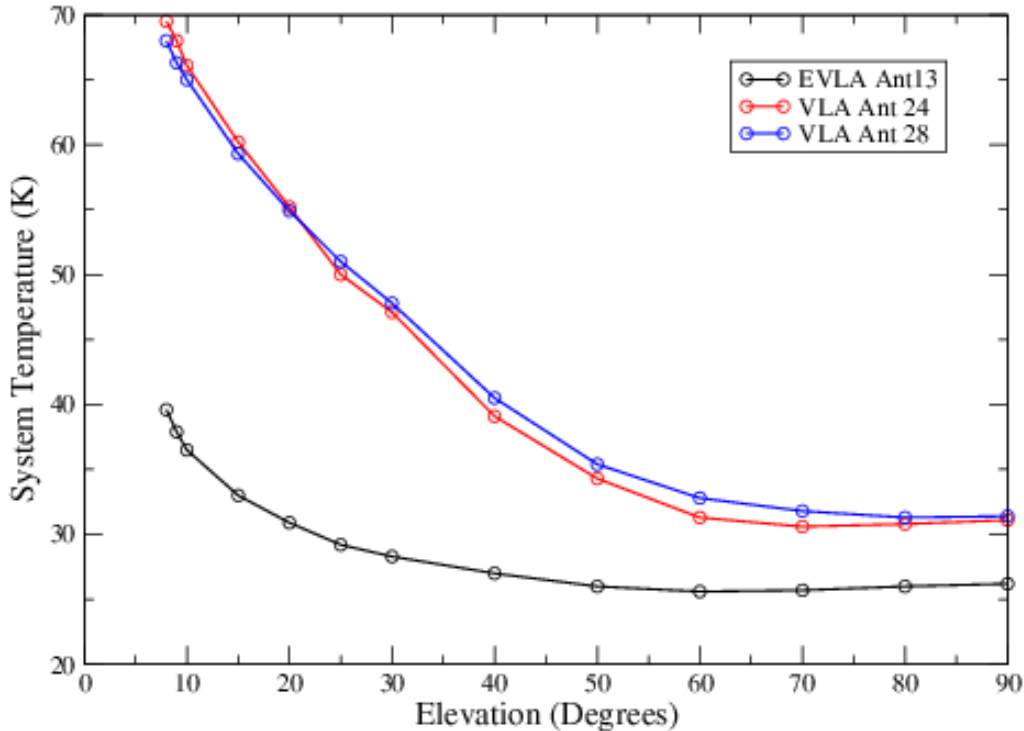


Figure 8: **EVLA System Temperature Variation with Elevation at L Band.** This plot displays the EVLA improvement in system temperature performance as a function of elevation at 1425 MHz. The blue and red lines are standard VLA antennas, while the more shallowly sloped black line is an EVLA antenna. For more details, see EVLA Memo No. 85, available on the web (see Section 6).

When using these coefficients, one must first correct for the opacity (typically measured using the TIPPER procedure), via the AIPS program CLCOR, then apply the gain coefficients in a subsequent run of CLCOR. The TIPPER procedure is an observing mode on the VLA which entails a simple measurement of the sky brightness as a function of elevation. The on-line software uses these data to derive the atmospheric zenith opacity and system temperature. This observing mode is known to the JObserve program. If no measurements were taken, it also is possible to derive an estimate of the opacity from seasonal averages or nearby observations (see <http://www.vla.nrao.edu/astro/calib/tipper/>). Contact Bryan Butler, Steve Myers, or Claire Chandler for advice on these techniques.

3.5 Field of View

At least four different effects will limit the field of view. These are: primary beam; chromatic aberration; time-averaging; and non-coplanar baselines. We discuss each briefly:

3.5.1 Primary Beam

The ultimate factor limiting the field of view is the diffraction-limited response of the individual antennas. An approximate formula for the full width at half power in arcminutes

is: $\theta_{\text{PB}} = 45/\nu_{\text{GHz}}$. More precise measurements of the primary beam shape have been derived and are incorporated in the AIPS task `PBCOR` to allow for correction of the primary beam attenuation in wide-field images. Objects larger than approximately half this angle cannot be directly observed by the array. However, a technique known as ‘mosaicing’, in which many different pointings are taken, can be used to construct images of larger fields. Refer to References 1 and 2 for details, or contact Debra Shepherd.

3.5.2 Chromatic Aberration (Bandwidth Smearing)

The principles upon which synthesis imaging are based are strictly valid only for monochromatic radiation. When radiation from a finite bandwidth is accepted and gridded as if monochromatic, aberrations in the image will result. These take the form of radial smearing which worsens with increased distance from the delay-tracking center. The peak response to a point source simultaneously declines in a way that keeps the integrated flux density constant. The net effect is a radial degradation in the resolution and sensitivity of the array.

These effects can be parameterized by the product of the fractional bandwidth ($\Delta\nu/\nu_0$) with the source offset in synthesized beamwidths ($\theta/\theta_{\text{HPBW}}$). Table 11 shows the decrease in peak response and the increase in apparent radial width as a function of this parameter.

Table 11: **Reduction in Peak Response Due to Bandwidth Smearing**

$\frac{\Delta\nu}{\nu_0} \frac{\theta_0}{\theta_{\text{HPBW}}}$	Peak	Width
0.0	1.00	1.00
0.50	0.95	1.05
0.75	0.90	1.11
1.0	0.80	1.25
2.0	0.50	2.00

Note: The reduction in peak response and increase in width of an object due to bandwidth smearing (chromatic aberration). $\Delta\nu/\nu_0$ is the fractional bandwidth; $\theta_0/\theta_{\text{HPBW}}$ is the source offset from the phase tracking center in units of the synthesized beam.

If you wish to obtain maximum sensitivity and resolution over the entire field-of-view of the antennas, then the spectral-line modes of the correlator (also known as multichannel continuum or pseudo-continuum) probably will be required.

3.5.3 Time-Averaging Loss

The sampled coherence function (visibility) for objects not located at the phase-tracking center is slowly time-variable due to the changing array geometry, so that averaging the samples in time will cause a loss of amplitude. Unlike the bandwidth loss effect described above, the losses due to time averaging cannot be simply parameterized. The only simple case exists for observations at $\delta = 90^\circ$, where the effects are identical to the bandwidth effect except they operate in the azimuthal, rather than the radial, direction. The functional dependence is the same in this case with $\Delta\nu/\nu_0$ replaced by $\omega_e \Delta t_{\text{int}}$, where ω_e is the Earth’s angular rotation rate, and Δt_{int} is the averaging interval.

For other declinations, the effects are more complicated and approximate methods of analysis must be employed. Chapter 13 of Reference 1 considers the average reduction in image amplitude due to finite time averaging. The results are summarized in Table

12, showing the time averaging in seconds which results in 1%, 5% and 10% loss in the amplitude of a point source located at the first null of the primary beam. These results can be extended to objects at other distances from the phase tracking center by noting that the loss in amplitude scales with $(\theta\Delta t_{\text{int}})^2$, where θ is the distance from the phase center and Δt_{int} is the averaging time. Since the size of VLA continuum data sets typically is not a limiting factor for modern computers, we recommend that most observers reduce the effect of time-average smearing by using integration times of $3\frac{1}{3}$ seconds (also see Section 3.6) in at least the **A** and **B** configurations.

Table 12: **Loss vs. Averaging Time for Time Averaging Smearing**

Configuration	Amplitude loss		
	1.0%	5.0%	10.0%
A	2.1	4.8	6.7
B	6.8	15.0	21.0
C	21.0	48.0	67.0
D	68.0	150.0	210.0

Note: The averaging time (in seconds) resulting in the listed amplitude losses for a point source at the antenna first null. Multiply the tabulated averaging times by 2.4 to get the amplitude loss at the half-power point of the primary beam. Divide the tabulated values by 4 if interested in the amplitude loss on the longest baselines.

3.5.4 Non-Coplanar Baselines

The procedures by which nearly all images are made in Fourier synthesis imaging are based on the assumption that all the coherence measurements are made in a plane. This is strictly true for E-W interferometers, but is false for the VLA, with the single exception of snapshots. Analysis of the problem shows that the errors associated with the assumption of a planar array increase quadratically with angle from the phase-tracking center. Serious errors result if the product of the angular offset in radians times the angular offset in synthesized beams exceeds unity. The effects are especially severe at the 90 cm and 400 cm bands, where standard two-dimensional imaging can be done only for **D**-configuration data. This effect is noticeable at $\lambda 20$ cm in certain instances, but can be safely ignored at shorter wavelengths.

A solution to the problem of imaging wide-field data taken with non-coplanar arrays is well known, and has been implemented in the AIPS program **IMAGR**. This program can now correctly image up to 512 subfields, sufficient to handle observations in the **B**, **C**, and **D** configurations. We expect that as computer performance continues to improve, full imaging of even **A** configuration data will soon be practical. Refer to the help file for this program, or consult with Rick Perley or Frazer Owen, for advice. More computationally efficient imaging with non-coplanar baselines is being investigated, such as the “W-projection” method; see EVLA Memo 67 for more details.

3.6 Time Resolution

The minimum integration time at which all data can be written is a function of the total number of channels of data produced by the correlator. This minimum time varies from $1\frac{2}{3}$ seconds for the continuum mode to 5 seconds for 512 channel spectral line modes. Note

that in order to ensure the complete removal of correlator offsets, averaging times should be an integer multiple of $3\frac{1}{3}$ seconds (which is the period of the Walsh functions that are used to negate cross-coupling between antenna signal lines).

Averaging times shorter than those listed above can be selected, but only at the cost of removing antennas from the array. For the spectral line modes, Table 13 gives the minimum allowed integration time as a function of the numbers of IFs and channels. In continuum mode, integration times as short as 0.4 seconds are available, but are appropriate only for EVLA testing and for fast flaring activity such as solar flares. Contact Ken Sowinski for details on their use.

Table 13: Minimum Integration Times for One Subarray of 27 Antennas

N_{ch}	1 IF	2 IFs	4 IFs
16	1-1/3 sec	1-2/3 sec	3-1/3 sec
32	1-1/3 sec	1-2/3 sec	3-1/3 sec
64	3-1/3	3-1/3	3-1/3
128	3-1/3	3-1/3	3-1/3
256	3-1/3	3-1/3	3-1/3
512	5	5	5

Note: The number of channels, N_{ch} , is the number of channels per IF multiplied by the number of IFs in Normal mode (Table 18). For Hanning smoothing multiply by another factor of 2.

The maximum recommended integration time for any VLA observing is 60 seconds, but given current computing capabilities there is no reason to use integration times longer than 10 seconds. For high frequency observers with short scans (e.g., fast switching, as described in Section 3.13.2), a $3\frac{1}{3}$ second integration time may be preferable.

Users should keep in mind the data rate of the VLA when planning their observing. The array’s maximum data rate of more than 3 GByte per day presently is only a minimal problem for the modern computers that most astronomers use for their data reduction. If necessary, this rate may be reduced by increasing the averaging time and/or decreasing the number of spectral channels. Consult one of the spectral line experts listed in Table 20 for advice. ‘

3.7 Radio-Frequency Interference

The bands within the tuning range of the VLA which are allocated exclusively to radio astronomy are 1400 – 1427 MHz, 1660 – 1670 MHz, 4990 – 5000 MHz, 15.35 – 15.4 GHz, 22.2 – 22.5 GHz, and 23.6 – 24.0 GHz. No external interference should occur within these bands. Experience shows that RFI is a serious problem only within the 20, 90, and 400 cm bands. At 20 cm, interference is most serious to the **D** configuration, as the fringe rates in other configurations are often sufficient to reduce interference to tolerable levels.

RFI at the VLA is an increasing problem to astronomical observations. To monitor this increase, and to provide a rough guide to the severity of this interference, the RFI spectrum at all bands from P through K is measured on an occasional basis, using the VLA correlator system. Plots of typical spectra in the L and P bands, taken with 6 kHz resolution, are shown in Figures 9 and 10.

Downloadable plots of all RFI observations from 1993 onwards are available on the

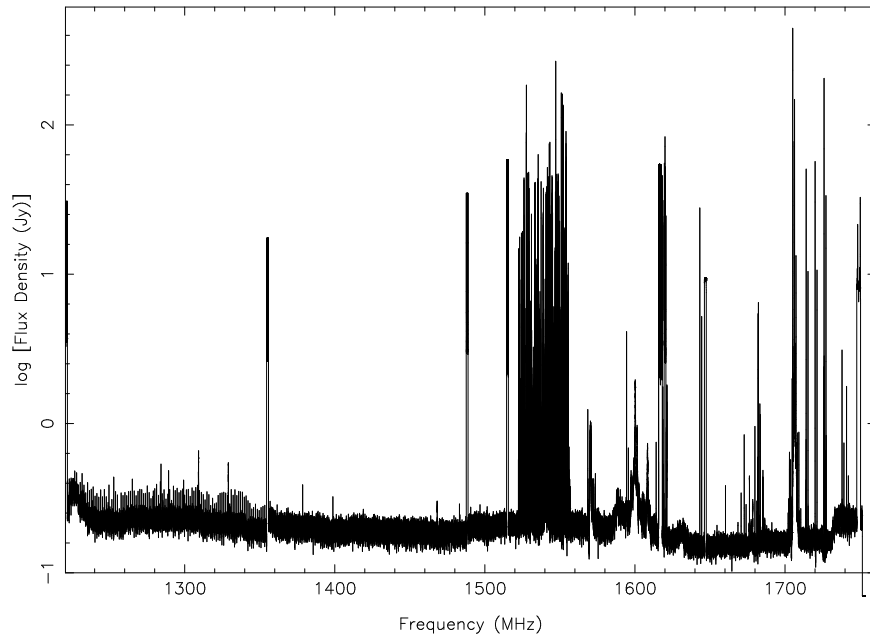


Figure 9: **Typical L-band interference Spectrum.**

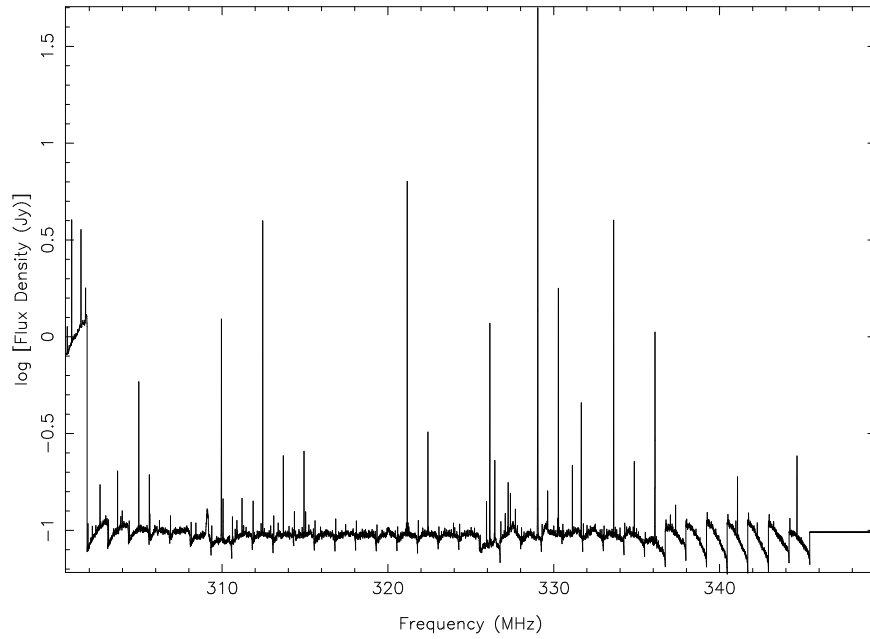


Figure 10: **Typical P-band Interference Spectrum.**

Web. For general information about the RFI environment, contact the head of the IPG (Interference Protection Group) by sending e-mail to NRAO-RFI@nrao.edu.

Table 14 is a convenient summary of eight such observations taken during 2001. This

Table 14: **VLA RFI Between 1260 and 1740 MHz**

Frequency	Avg. Flux	Pk. Flux	Source	Comments
1277 MHz	12 mJy	20 mJy	Aerostat Radar	Sometimes absent
1286	2	5	Farmington Radar	Other weak lines nearby
1300	2	5	Internal RFI	
1310	100	100	ABQ Radar	
1316	???	???	ABQ Radar	Weaker, often absent
1330	45	80	ABQ Radar	Sometimes absent
1381	3	100	GPS L3 IONDS	On < 3% of the time
1400	60	60	Internal RFI	
1429-1435	15	130	Military	Four separate lines
1444,1453	5	> 100	High Altitude Balloons	NASA/NSBF
1500	2	5	Internal RFI	
1515	15	> 100	High Altitude Balloons	
1525	6	> 100	High Altitude Balloons	
1530-1544	> 130	> 200	INMARSAT	Many ‘lines’
1557-1567	10	20	GPS Sidelobe?	Wide spectrum
1570-1580	> 500	> 500	GPS-L2	Wide spectrum
1600	120	120	Internal RFI	
1602-1616	> 500	> 500	GLONASS	Many separate ‘lines’
1610-1645	>500	>500	IRIDIUM!	See text
1620	80	300	?	
1650	13	25	Internal RFI	
1678-1698	50	100	Radiosondes, satellite	> 6 variable ‘lines’.
1710	10	10	?	

table lists the ‘line’ frequency, the average equivalent flux density (in mJy) in 50 MHz, and the peak flux density, also reduced to 50 MHz equivalent bandwidth. A significant difference between these columns indicates that the RFI is intermittent. These equivalent flux densities are approximate, and should be used only to give a rough approximation to the severity and likelihood of a problem. A more detailed version of Table 14 is available on the web at <http://www.vla.nrao.edu/astro/rfi/rifreqs.txt>.

Between 1220 and 1255 MHz, very strong and very broad RFI is always present, primarily due to the GPS-L2 signal at 1227.6 ± 10 MHz, and a border radar at 1252 ± 1.25 MHz near Deming, New Mexico. It may be possible to observe in selected, narrow bandwidths in this region. Numerous other strong radars belonging to the FAA’s Air Route Surveillance system exist between 1250 and 1350 MHz in the general vicinity of the VLA. Between 1435 and 1530 MHz, aeronautical telemetry from White Sands Missile Range (WSMR) occasionally will interfere with observing. These transmissions are very occasional, and unpredictable. They are worst in the spring, during the WSMR wargames exercises. Above 1700 MHz, communications equipment previously used by the US Forest Service has largely been decommissioned, and the spectrum in this region now is much cleaner than it was previously.

Note that the listed RFI signal strengths are appropriate for the **D** configuration. These signal strengths are considerably reduced in the larger configurations – an average attenu-

ation of perhaps a factor of 100 will be obtained in the **A** configuration due to fringe phase winding.

In late 1998, the Iridium constellation of Low Earth Orbit (LEO) satellites was activated. As is well known, this venture was not a commercial success, but it was purchased by a consortium of investors called Iridium LLC, and is being operated by Boeing. Thus these satellites are still broadcasting in the 1621–1627 MHz band, but their signals are strong enough that VLA observations between 1610 and \sim 1645 MHz generally are not possible. Filters have been installed to allow 1612 MHz OH observations (see <http://www.vla.nrao.edu/astro/guides/ifilt/>).

In general, it may be possible to observe in spectral regions containing strong RFI provided: (1) That the RFI is not so strong as to cause serious gain compression in the amplifiers, and (2) That the RFI is kept out of the correlator through use of a narrow back-end filter. This latter requirement is particularly important for spectral line correlator modes, although use of Hanning smoothing is very effective in reducing the Gibbs ringing (described in the VLA Spectral Line Users Guide, at <http://www.vla.nrao.edu/astro/guides/sline/current/>). Gain compression in the antenna electronics often can be prevented by using a narrower (12.5 or 25 MHz) “front-end” filter (actually present in the IF stage), rather than the default 50 MHz filter. Note that use of these FE filters greatly restricts the range of tunable frequencies. The scheduling program **JObserve** is aware of these restrictions, and should be used when contemplating use of the narrow front-end filters.

Observers can use Table 14 to assist in deciding which center frequencies and bandwidths are most likely to result in good data at L band. There are very few good combinations for 50 and 25 MHz bandwidths. These are summarized in Table 15, which shows the ‘statistically’ best frequencies to use at L-band with the listed bandwidths. Note that the VLA LO system restricts the selection of frequencies at both 50 MHz and 25 MHz bandwidths. The restrictions are particularly severe at a bandwidth of 50 MHz – for a given IF, the only center frequencies (in MHz) which can be observed with that bandwidth are those ending in 15, 35, 65, or 85. (For example, between 1400 and 1500 MHz, the only permitted frequencies are 1415, 1435, 1465 and 1485 MHz.) With the 25 MHz front-end bandwidth filters, regions 5 MHz wide centered on 1250, 1300, 1350, . . . , cannot be tuned. And when using the 12 MHz front-end bandwidth filters, 8 MHz wide regions centered at 1225, 1275, 1325, 1375, . . . , and 18 MHz wide regions centered at 1250, 1300, 1350, 1400, . . . , cannot be reached.

Table 15: **Recommended Center Frequency/Bandwidth Combinations for L Band**

BW	Class A No RFI Expected	Class B Weak/Occas'l RFI	Class C 'Tolerable' RFI
50 MHz	none	1365,1435,1465,1485	1335,1385,1415
25 MHz	1343 – 1347 1353 – 1387 ⁽¹⁾ 1413 – 1417 1663 – 1665	1290 – 1297 1453 – 1470 1503 – 1517	Use Table 14

Footnotes:

1. The White Sands Missile Range uses 1357 ± 3 MHz for airborne telemetry once or twice per week.

The ubiquity of L-band interference makes it difficult for users wishing high sensitivity to find significant bandwidths free of RFI. As a result of monitoring the RFI, we have established a number of standard bands which are more likely to be free of significant RFI. These are shown below in Table 16.

Table 16: JObserve Names of L-band ‘Standard Frequencies’

JObserve Name	AC		BD	
	Center Frequency	Bandwidth	Center Frequency	Bandwidth
LL	1464.9	50	1385.1	50
L1 ⁽¹⁾	1364.9	50	1435.1	50
L2	1515.9	25	1365.1	25
L3	1515.9	25	1435.1	25

Footnotes:

1. The L1 frequency combination was used for the NVSS and FIRST surveys.

Another important form of RFI consists of signals which are generated by each antenna. These signals are picked up by nearby antennas, or by the generating antenna’s feed, and produce correlated signals in the visibility data. This form of RFI is especially important in the P and 4 bands when in the C and D configurations. They appear at all multiples of 5 and 12.5 MHz - frequencies divisible by these numbers must be avoided. (It is this spectrum of RFI which limits our P-band bandwidth to 3.125 MHz.) Another family of RFI occurs at multiples of 100 kHz - these are much weaker and can be ignored for continuum work at 90 cm, but are important on many baselines at the 400 cm band.

At P band, the RFI situation can be particularly difficult. Interference is relatively infrequent in the evenings and on weekends, but during the day, very strong interference – sufficient to saturate the receivers – is common. The best advice is to arrange observing to fall outside of regular working hours. Very sensitive spectral line observations at P band require special measures at the VLA site to turn off known sources of RFI. To implement these measures, contact the interference protection group (see Table 20). The situation at 4 band generally is better, as nearly all of the RFI is weak and is generated by the antennas themselves (see above); the self-generated RFI can be removed in processing provided the spectral line correlator mode is employed.

At P and 4 bands, use of the spectral line correlator modes is strongly recommended for all observations to allow diagnosis and removal of internal and external interference. For observations which do not require linear polarization information, use of the correlator modes ‘1x’, ‘2xy’, or ‘4’ is recommended to maximize the spectral resolution. The labels ‘x’ and ‘y’ are the IF designators, A, B, C, or D. Refer to Section 2 for a description. The current default for 327 MHz is now ‘4’.

For L, C, K, and Q bands, observers should avoid using an L6 (second LO) setting of 3760 or 3790 MHz, due to an internal birdie produced by those LO settings. For X and U bands, avoid using 3840 and 3810 MHz. The JObserve program is aware of these restrictions, so users should not inadvertently fall victim to this problem.

3.8 Antenna Pointing

The pointing parameters of the antennas are measured monthly under calm nighttime conditions. The antenna model, using these parameters, suffices under good weather to allow blind pointing to an accuracy of about 10 arcsec rms. The pointing accuracy in daytime is a little worse, due to the effects of solar heating of the antenna structures.

Moderate winds have a very strong effect on both pointing and antenna figure. The advertised maximum wind speed for precision operations is 15 mph (7 m/s), and careful observations have demonstrated this to be the practical maximum wind speed for useful observing at K and Q bands. Observations at these bands in winds significantly in excess of this limit are not advisable, and users should consider moving to a lower frequency. Wind speeds near the stow limit (45 mph) will have a similar negative effect at X and U bands.

To achieve better pointing, we have added a capability for repeated calibration and correction of the local pointing error during astronomical observations. In this observing mode, known as ‘referenced pointing’, a nearby calibrator is observed in interferometer pointing mode every hour or so. The local pointing corrections thus measured can then be applied to subsequent target observations. Tests show that this mode reduces rms pointing errors to typically 2 – 3 arcseconds if the reference source is within about 10 degrees (in azimuth and elevation) of the target source, and the source elevation is less than 70 degrees. The `JObserve` program is aware of this observing mode.

Use of referenced pointing is highly recommended for all K- and Q-band observations, and for X- and U-band observations of objects whose total extent is a significant fraction of the antenna primary beam. It is usually recommended that the referenced pointing measurement be made at X-band, regardless of what band your target observing is at, since X-band is the most sensitive, and the closest calibrator is likely to be rather weak. Proximity of the reference calibrator to the source position is of paramount importance. The calibrator should have at least 300 mJy flux density and be unresolved on all baselines to ensure an accurate solution.

Measuring the pointing offsets at K-band for subsequent K-band observing is usually successful, but should not be attempted on objects of less than 300 mJy flux density. However, attempting to measure these offsets at Q-band directly generally is not recommended, since the blind pointing error is often larger than the Q-band half-power half-width – which will cause the referenced pointing to fail.

Secondary referenced pointing (*i.e.*, using X-band referenced pointing to permit subsequent Q-band or K-band determination of the residual pointing errors), is recommended only for high precision observations at Q and K bands when observing extended objects which fill the antenna primary beam. For general observing of small objects, simple referenced pointing using the offsets determined at X-band is nearly always sufficient to keep all antennas pointing to within 5 arcseconds.

Consult with Rick Perley, Ken Sowiński, or Claire Chandler for more information about referenced pointing. The information above is largely taken from the guide to high-frequency observing on the VLA, found at <http://www.vla.nrao.edu/astro/guides/highfreq/>.

3.9 Subarrays

The VLA can simultaneously process five different observing programs if they are fixed-scheduled, or two if they are dynamically-scheduled. However, the subarrays are not all fully independent. If use of this capacity is contemplated, the following limitations must be

understood and followed:

1. Each subarray uses a different observing file. The VLA operator must be told which file is to control which subarray, and which antennas are to be in each subarray. Once observing has begun, antennas should not be reassigned from one subarray to another. The subarray with the largest number of antennas is designated the “majority subarray”.
2. All correlator parameters, including integration time, bandwidth, number of channels, etc., are determined by that requested in the observe file for the majority subarray. Any correlator settings requested in the observe files for other subarrays will be ignored.
3. There are only two sets of Fluke synthesizers (the final LOs in the frequency conversion system for the VLA) – hence, only two subarrays can have completely independent frequency selection if they include VLA antennas. Most experiments are likely to have all remaining VLA antennas in the same subarray, but if VLA antennas need to be included in more than one subarray please contact Ken Sowinski or Bryan Butler.

Single-antenna (or multiple-antenna) VLBI programs cause special problems. Such programs use one of the Fluke sets, leaving only one for the remaining four subarrays – these must then share that single Fluke set, or use the same values assigned to the VLBI run. Generally, VLBI Fluke settings are compatible with continuum observing. Fortunately, the correlator restrictions listed above (point 2) do NOT apply to the single-antenna VLBI subarrays.

3.10 Positional Accuracy

The accuracy with which an object’s position can be determined is limited by the atmospheric phase stability, the closeness of a suitable (astrometric) calibrator, and the calibrator-source cycle time. Under good conditions, in **A** configuration, accuracies of about 0.05 arcseconds can be obtained. Under more normal conditions, accuracies of perhaps 0.1 arcseconds can be expected. Under extraordinary conditions (probably attained only a few times per year on calm winter nights in **A** configuration when using rapid phase switching on a nearby astrometric calibrator – see Section 3.13.2), accuracies of 1 milliarcsecond have been attained.

If highly accurate positions are desired, only ‘A’ code (astrometric) calibrators from the VLA Calibrator List should be used. The positions of these sources are taken from lists published by the USNO.

3.11 Limitations on Imaging Performance

Imaging performance can be limited in many different ways. Some of the most common are listed in the following subsections. There are particular limitations of the hybrid VLA-EVLA systems. Some of these are described below, but the cautious observer should consult <http://www.vla.nrao.edu/astro/guides/evlareturn/> for a complete discussion.

3.11.1 Image Fidelity

With conventional point-source calibration methods, and even under the best observing conditions, the achieved dynamic range will rarely exceed a few hundred. The limiting factor is the atmospheric phase stability. If the target source contains more than 50 mJy⁵ in compact structures (depending somewhat on band), self-calibration can be counted on in improving the images. Dynamic ranges in the thousands can be achieved using these techniques. At this level, the limitations are generally due to errors in the calculation of the correlation coefficient (‘closure’ errors). Recent (1998) software changes in the VLA’s calculation of these coefficients have dramatically reduced the level of these errors for VLA-only continuum observing, particularly for the narrower bandwidths where these errors were larger.

If the target source is bright enough for dynamic ranges exceeding 10,000 (based on peak/rms thermal noise) to be conceivable, use of one of the spectral line correlator modes should be considered, since the correlator errors which limit the dynamic range are greatly reduced. However, due to inherent limitations in correlator capacity, this will necessarily require a reduction in bandwidth by a factor of at least four. If the target source is only slightly resolved, use of the continuum mode with phased array observing will reduce the ‘closure’ errors without loss of bandwidth.

3.11.2 VLA-EVLA Closure Errors

Antenna calibration algorithms generally assume that calibration quantities (both in the antennas and in the atmosphere) can be separated on an antenna-by-antenna basis. This provides substantial strength in determining calibration quantities, since (for 27 antennas) 351 baselines of interferometer visibility data may be used to determine 27 individual calibration values, one for each antenna. However, this assumption breaks down for a mixed array of VLA antennas and retrofitted EVLA antennas, since the improved EVLA bandpass response functions are not matched exactly to the poorer (but identical to each other) bandpass responses of VLA antennas. A symptom of the breakdown of this assumption is excessive amplitude closure errors when running the AIPS task CALIB, where the VLA-VLA baselines (or EVLA-EVLA baselines, for data where the number of VLA antennas exceeds those of the EVLA) may be reported to have closure errors as high as 8% for 50 MHz bandpasses, or even larger for narrower bandpasses. The closure errors originate in the mismatch of the VLA-EVLA bandpasses and the CALIB assumption that all calibration quantities are antenna-based, and the ultimate result is a miscalibration of the VLA-VLA baselines. For continuum observations, the closure errors may be calibrated by observing a strong calibrator and solving for baseline-dependent errors using the AIPS task BLCAL. For spectral-line observations, the standard bandpass calibrations (e.g., AIPS task BPASS) also will remove the effects of the mismatched bandpasses.

3.11.3 Invisible Structures

An interferometric array acts as a spatial filter, so that for any given configuration, structures on a scale larger than the fringe spacing of the shortest baseline will be completely absent. Diagnostics of this effect include dark bowls around extended objects, and large-

⁵This limiting successful flux density can be considerably lower, if the atmospheric coherence time is many minutes, or higher, for short coherence times and noisier frequencies

scale stripes in the image. Table 4 gives the largest scale visible to each configuration/band combination.

3.11.4 Poorly Sampled Fourier Plane

Unmeasured Fourier components are assigned values by the deconvolution algorithm. While this often works well, sometimes it fails noticeably. The symptoms depend upon the actual deconvolution algorithm used. For the CLEAN algorithm, the tell-tale sign is a fine mottling on the scale of the synthesized beam, which sometimes even organizes itself into coherent stripes. Further details are to be found in Reference 1.

3.11.5 Sidelobes from Confusing Sources

At 90 and 20 cm, large numbers of background sources are located throughout the primary antenna beam. Sidelobes from these objects will lower the image quality of the target source. Although bandwidth and time-averaging will tend to reduce the effects of these sources, the very best images will require careful imaging of all significant background sources. The AIPS task IMAGR is well suited to this task at 20 cm. The problem at 90 cm is much worse, and is greatly complicated by the non-coplanar nature of the array, as described in Section 3.5.4. Table 4 gives the highest flux density expected of these background sources, and the total background flux density. Note that there is an NVSS RUN file generator (available from the NVSS page at <http://www.cv.nrao.edu/nvss/>) that can be extremely helpful in defining the fields containing confusing sources.

3.11.6 Sidelobes from Strong Sources

Another image-degrading effect is that due to strong nearby sources. Again, the 20 and 90 cm bands are especially affected. The active Sun will be visible to any **D** configuration daytime spectral line observation at these bands. Even with 50 MHz bandwidth in continuum mode, the active Sun can ruin the short spacings of observations within about 20 degrees of the Sun. The quiet Sun poses a lesser threat, so the general rule is to go ahead and observe, even if the target source is close to the Sun. At 90 and 400 cm, observations within approximately 10 degrees of Cygnus A, Cassiopeia A, Taurus A, and Virgo A will be greatly degraded.

3.12 Calibration and the Flux Density Scale

The VLA Calibrator List contains information on 1860 sources sufficiently unresolved and bright to permit their use as calibrators. Copies of the list are distributed throughout the DSOC. The list is also available within the JObserve program and may be accessed on the Web at <http://www.vla.nrao.edu/astro/calib/manual/>.

Accurate flux densities can be obtained by observing one of 3C286, 3C147, 3C48 or 3C138 during the observing run. Not all of these are suitable for every observing band and configuration – consult the VLA Calibrator Manual for advice. Over the last several years, we have implemented accurate source models directly in AIPS for much improved calibration of the amplitude scales; see page 21 of the July 2006 NRAO Newsletter for details. At present, models are available for 3C48 and 3C286 for all bands from 1.3 to 20 cm, for 3C138 at all bands from 1.3 to 6 cm, and for 3C147 at all bands from 0.7 to 2.0 cm.

Since the standard source flux densities are slowly variable, we monitor their flux densities when the VLA is in its **D** configuration. As the VLA cannot measure *absolute* flux densities, the values obtained must be referenced to assumed or calculated standards, as described in the next paragraph. Table 17 shows the flux densities of these sources in November 2001 at our standard bands. The accuracy of these values, relative to the assumed standards, is set by the gain stability of the VLA. The estimated 1- σ errors in the table, relative to the assumed standards, are less than 1% for frequencies up to 25 GHz, and about 2% for the 43 GHz band.

The flux densities shown in the table for frequencies below 10 GHz are based on the Baars *et al.* value for 3C295. For frequencies above 10 GHz, the flux densities are based on models of Mars and NGC 7027 which are themselves based on the Baars scale below 10 GHz.

Polynomial coefficients describing the derived flux densities for the standard calibrators have been determined which permit accurate interpolation of the flux density at any VLA frequency. These coefficients are updated approximately every few years, and are implemented into the AIPS task SETJY. At present, a substantial new effort is under way to improve the long-term (past and present) accuracy of the VLA flux density scale; contact Rick Perley or Bryan Butler for information on this work. Although final information is not yet available, it appears that the flux densities of 3C48 and 3C286 relative to 3C295 have changed by less than 1% over the last 25–30 years.

Table 17: **Flux densities (Jy) of Standard Calibrators for November 2001**

Source/Frequency (MHz)	327.5	1465	4885	8435	14965	22460	43340
3C48 = J0137+3309	45.52	15.54	5.47	3.22	1.83	1.23	0.63
3C138 = J0521+1638	19.34	8.16	3.71	2.43	1.54	1.10	0.62
3C147 = J0542+4951	55.00	21.32	7.88	4.72	2.77	1.93	1.11
3C286 = J1331+3030	25.96	14.49	7.49	5.22	3.51	2.63	1.58
3C295 = J1411+5212	60.37	21.49	6.53	3.42	1.67	0.99	0.41
NGC7027	<0.2	1.54	5.52	6.03	5.90	5.68	5.22
MARS	–	–	0.175	0.528	1.67	3.81	14.22

For most observing projects, the effects of atmospheric extinction will automatically be accounted for by regular calibration when using a nearby point source whose flux density has been determined by an observation of a flux density standard taken at a similar elevation. However, at high frequencies (most notably K-band, Ka-band, and Q-band), both the antenna gain and the atmospheric absorption may be strong enough to make ‘simple’ flux density bootstrapping unreliable. The AIPS task ELINT is now available to permit measurement of an elevation gain curve using your own observations, and subsequent adjustment of the derived gains to remove these elevation-dependent effects. The current calibration methodology does not require knowledge of the atmospheric extinction (since the true flux densities of the standard calibrators are believed known). However, if knowledge of the actual extinction is desired, a simple antenna tipping procedure is available (and is known to the JObserve program) which will provide both the vertical extinction and the total system temperature. For advice on these procedures, contact Bryan Butler, Rick Perley, or Claire Chandler.

3.13 Phase Calibration

3.13.1 General Guidelines for Phase Calibration

Adequate phase calibration is a complicated function of source-calibrator separation, frequency, array scale, and weather. And, since what defines adequate for some experiments is completely inadequate for others, it is impossible to define any simple guidelines to ensure adequate phase calibration in general. However, some general statements remain valid most of the time. These are given below.

- Tropospheric effects dominate at wavelengths shorter than 20 cm, ionospheric effects dominate at wavelengths longer than 20 cm.
- Atmospheric (troposphere and ionosphere) effects are nearly always unimportant in the **C** and **D** configurations at L and P bands, and in the **D** configuration at X and C bands. Hence, for these cases, calibration need only be done to track instrumental changes – once per hour is generally sufficient.
- If your target object has sufficient flux density to permit self-calibration, there is no need to calibrate more than once hourly.
- The smaller the source-calibrator angular separation, the better. In deciding between a nearby ‘S’ calibrator, and a more distant ‘P’ calibrator, the nearby calibrator is usually the better choice.
- At high frequencies, and longer configurations, rapid switching between the source and nearby calibrator is often helpful. See the following section.

3.13.2 Rapid Phase Calibration and the Atmospheric Phase Interferometer (API)

For some objects, and under suitable weather conditions, the phase calibration can be considerably improved by rapidly switching between the source and calibrator. An observing technique denoted ‘fast switching’ has been developed to more conveniently permit the user to implement this methodology. Source-Cal observing cycles as short as 40 seconds can now be used – such a short cycle is impossible with traditional VLA observing techniques.

This method is not for everyone! Considerable integration time is lost with very short cycle times, so it is important to balance this certain loss against a realistic estimate of the possible gain. Experience has shown that cycle times of 100 to 150 seconds at high frequencies have been effective for source-calibrator separations of less than 10 degrees. The fast switching technique ‘stops’ tropospheric phase variations at an effective baseline length of $\sim v_a t/2$ where v_a is the atmospheric wind velocity aloft (typically 10 to 15 m/sec), and t is the total switching time. This technique has been demonstrated to result in images of faint sources with diffraction-limited spatial resolution on the longest VLA baselines. Under average weather conditions, and using a 120 second cycle time, the residual phase at 43 GHz should be reduced to ≤ 30 degrees. Further details can be found in VLA Scientific Memos # 169 and 173. These memos, and other useful information, can be obtained from Reference 12 in Section 6.

The fast switching system has been implemented in the current version of the **JObserve** program. Note that the technique will not work in bad weather (such as rain showers, or when there are well-developed convection cells – most notably, thunderstorms). Contact

Claire Chandler or Chris Carilli for details and advice, and see the high-frequency observing guide at <http://www.vla.nrao.edu/astro/guides/highfreq/>.

The NRAO Atmospheric Phase Interferometer (API) is now operational at the VLA, and software has been installed for real time monitoring of the phase stability through the web. A detailed description of the API, and instructions for accessing its data, may be found at <http://www.vla.nrao.edu/astro/guides/api/>. The API continuously measures the tropospheric contribution to the interferometric phase using an interferometer comprised of two 1.5 meter antennas separated by 300 meters, observing an 11.3 GHz beacon from a geostationary satellite. The API data can be used to estimate the required calibration cycle times when using fast switching phase calibration, and in the worst case, to indicate to the observer that high frequency observing may not be possible with current weather conditions. Contact Chris Carilli for further details.

3.14 Polarization

The continuum correlator mode provides full polarimetric information for both observing frequencies. The polarimetric spectral line modes (PA and PB) are also available for observations of linearly polarized spectral lines, or for observations of continuum objects where large field-of-view or high dynamic range is necessary. Spectral line modes ‘2AC’, ‘2BD’, and ‘4’ do not provide linear polarization information.

For each observation requiring polarization information, the instrumental polarization should be determined through observations of a bright calibrator source spread over a range in parallactic angle. In nearly all cases, the phase calibrator chosen can double as a polarization calibrator. The minimum condition that will enable accurate polarization calibration is four observations of a bright source spanning at least 90 degrees in parallactic angle. The accuracy of polarization calibration is generally better than 0.5% for objects small compared to the antenna beam size. At least one observation of 3C286 or 3C138 is required to fix the absolute position angle of polarized emission. 3C48 also can be used to fix the position angle at wavelengths of 6 cm or shorter. The results of a careful monitoring program of these and other polarization calibrators will be found at <http://www.vla.nrao.edu/astro/calib/polar/>.

High sensitivity linear polarization imaging may be limited by time dependent instrumental polarization, which can add low levels of spurious polarization near features seen in total intensity and can scatter flux throughout the polarization image, potentially limiting the dynamic range. The instrumental polarization averaged among all baselines can vary by 0.3% on timescales of minutes to hours, limiting the believable fractional polarization to about 0.1%.

Wide field linear polarization imaging will be limited by the instrumental polarization beam. For a snapshot observation, the spurious linear polarization (after the standard polarization correction for the on-axis polarization response is applied) is $< 1\%$ at angles less than $\lambda/4D$ radians (D is the antenna diameter), is 1 – 3% at $\lambda/2D$, and increases sharply beyond this, reaching 10% at $3\lambda/4D$. Since the instrumental polarization response is directed radially and rotates with parallactic angle, the spurious polarization will tend to average down for long integrations. However, if the object being observed is very bright, and has a low degree of linear polarization, errors in the polarization calibration will cause Stokes I flux to be scattered into the Q and U images, thus limiting the polarization dynamic range.

Ionospheric Faraday rotation is always present at 20 cm and 90 cm. The typical

daily maximum rotation measure under quiet solar conditions is 1 or 2 radians/m², so the ionospheric-induced rotation of the plane of polarization at these bands is not excessive – 5 degrees at 20 cm, and perhaps 90 degrees at 90 cm. However, under active conditions, this rotation can be many times larger, such that accurate polarimetry is impossible at 20 cm.

The AIPS program TECOR has been shown to be quite effective in removing large-scale ionospheric-induced Faraday Rotation. It uses currently-available data in IONEX format. Please consult the TECOR help file for detailed information.

Circular polarization measurements are limited by the beam squint – the RCP and LCP primary beams are separated by 6 percent of the beamwidth along the axis perpendicular to the azimuth of the secondary focus feed position. Since circular polarization is determined from the difference between RCP and LCP signals, there results an appreciable error in all measurements of circular polarization off the pointing axis. The effect is large – the apparent circular polarization is ~10% at $\lambda/4D$, and ~20% at $\lambda/2D$. This false circular polarization is antisymmetric with respect to the center of the antenna beam, so 12-hour observations should partially cancel out the effect – however, even so, the residual apparent circular polarization is probably only accurate to a few percent.

Observers should be aware that detailed polarization tests have not yet been carried out for the retrofitted EVLA antennas. In particular, we expect that the VLA-EVLA baselines may have non-closing calibration problems similar to the total-intensity calibration (see Section 3.11). In addition, the interim EVLA receivers generally have poor polarization performance outside the frequency range previously covered by the VLA (e.g., outside the 4.5–5.0 GHz frequency range for C band), and the wider frequency bands of these interim receivers may be useful only for total intensity measurements.

3.15 Spectral Line Modes

The VLA correlator is very flexible, and can provide data in many ways. The various spectral line modes currently available are shown in Tables 18 and 19 and described below. **Users should note that these modes will become obsolete when the VLA correlator is decommissioned in early 2010, and will be replaced by new options and methods for specifying correlator setups.**

Most spectral line modes are distinguished by a code comprising a number followed by zero, one, or two letters. The number refers to the number of spectra being produced; the letters describe which IF channels are involved. Recall that each VLA antenna returns four signals: these are the RCP and LCP for each of two separately tuned frequencies. These signals are referred to as *IFs*, and are named A, B, C, and D. The first two represent RCP, and latter two LCP. IFs A and C are at one frequency (and cannot be different); B and D are at another (and also must be the same). In normal usage, the AC pair and the BD pair are at different frequencies within the same band. The spectral line modes can subdivide these IFs into 4 to 512 units, evenly spaced in frequency across the bandwidth of the input IF. These narrower units are referred to as *spectral line channels*. In addition to these interferometric spectra, autocorrelation spectra for all antennas are produced.

The single-IF modes provided by the spectral line correlator are known as 1A, 1B, 1C, and 1D. In these modes, only one spectrum is produced. These modes give the highest spectral resolution at any given bandwidth. The dual-IF modes are denoted 2AB, 2AC, 2AD, 2BC, 2BD and 2CD, and provide spectral information for the two IFs named (*e.g.* mode 2AC provides AA and CC correlations). Linear polarization measurements are not

Table 18: Available Bandwidths and Numbers of Spectral Line Channels in Normal Mode

BW Code	Bandwidth MHz	Single IF Mode ⁽¹⁾		Two IF Mode ⁽²⁾		Four IF Mode ⁽³⁾	
		No. Channels ⁽⁴⁾	Freq. Separ. kHz	No. Channels ⁽⁴⁾ per IF	Freq. Separ. kHz	No. Channels ⁽⁴⁾ per IF	Freq. Separ. kHz
0	50	16	3125	8	6250	4	12500
1	25	32	781.25	16	1562.5	8	3125
2	12.5	64	195.313	32	390.625	16	781.25
3	6.25	128	48.828	64	97.656	32	195.313
4	3.125	256	12.207	128	24.414	64	48.828
5	1.5625	512	3.052	256	6.104	128	12.207
6	0.78125	512	1.526	256	3.052	128	6.104
8	0.1953125	256	0.763	128	1.526	64	3.052
9	0.1953125	512	0.381	256	0.763	128	1.526

Footnotes:

1. Observing Modes 1A, 1B, 1C, 1D.
2. Observing Modes 2AB, 2AC, 2AD, 2BC, 2BD, 2CD.
3. Observing Modes 4, PA, PB. Note that modes PA and PB only provide correlations for a single IF pair (A & C for mode PA, or B & D for mode PB). Mode 4 provides correlations from both IF pairs (A & C and B & D), but without any cross hand correlation products. It is possible to use the output from one, two or four IFs in such a way as to obtain different combinations of number of spectral line channels and channel separation. The minimum and maximum number of channels is 4 and 512 respectively.
4. These are the numbers of spectral line channels produced in the array processor. Any number of spectral line channels that is a power of 2, that is less than or equal to the number in the table and that is greater than or equal to 2 may be selected using the data selection options available within the `JObserve` program.

possible with these modes, but circular polarization can be determined using the 2AC and 2BD modes. The four-IF modes are known as 4, PA and PB. The first of these provides spectra for all four IFs. Circular, but no linear polarization measurements are possible in this mode. The other two modes provide full polarimetric information – PA provides this for the A and C IFs (that is, it performs the correlations AA, AC, CA, and CC, providing a spectrum for each), PB for the B and D IFs. For the 4IF modes very few channels are available at the widest bandwidths and the bandpass formed has high spectral sidelobes. These sidebands will cause non-closing errors on sources distant from the delay tracking center. It is believed that modes PA and PB with 50 MHz bandwidth are unusable for any practical case. Whether a 25 MHz bandwidth is usable or not depends on the complexity of the field imaged and the required dynamic range. For the polarimetric modes, the descriptor 4 is omitted. The characteristics of all of these modes are summarized in Tables 18 and 19.

Correlator modes 2AB, 2AD, 2BC, 2BD, and 4 allow the IFs to use different bandwidths as well as to be tuned to different frequencies within the same band (e.g., mode 2AB will permit the AA correlations to be at a different frequency and bandwidth than the BB correlation). There are other restrictions. See Section 3.9, and the Spectral Line Users' Guide (listed in Chapter 6) for details.

Of central interest to observers is the stability of the spectra. Spectral line dynamic range is commonly defined as the ratio of the peak brightness in the strongest channel to

Table 19: Available Bandwidths and Numbers of Spectral Line Channels in Hanning Smoothing Mode

BW Code	Bandwidth MHz	Single IF Mode ⁽¹⁾		Two IF Mode ⁽²⁾		Four IF Mode ⁽³⁾	
		No. Channels ⁽⁴⁾	Freq. Separ. kHz	No. Channels ⁽⁴⁾ per IF	Freq. Separ. kHz	No. Channels ⁽⁴⁾ per IF	Freq. Separ. kHz
0	50	8	6250	4	12500	2	25000
1	25	16	1562.5	8	3125	4	6250
2	12.5	32	390.625	16	781.25	8	1562.5
3	6.25	64	97.656	32	195.313	16	390.625
4	3.125	128	24.414	64	48.828	32	97.656
5	1.5625	256	6.104	128	12.207	64	24.414
6	0.78125	256	3.052	128	6.104	64	12.207
8	0.1953125	128	1.526	64	3.052	32	6.104
9	0.1953125	256	0.763	128	1.526	64	3.052

Footnotes:

1. Observing Modes 1A, 1B, 1C, 1D.
2. Observing Modes 2AB, 2AC, 2AD, 2BC, 2BD, 2CD.
3. Observing Modes 4, PA, PB. Note that modes PA and PB only provide correlations for a single IF pair (A & C for mode PA, or B & D for mode PB). Mode 4 provides correlations from both IF pairs (A & C and B & D), but without any cross hand correlation products.
4. These are the numbers of spectral line channels produced in the array processor. Any number of spectral line channels that is a power of 2, that is less than or equal to the number in the table, and that is greater than or equal to 2 may be selected using the data selection parameters available in the `OBSERVE` and `JObserve` programs.

the minimum detectable line brightness in an image. This ratio is limited by instrumental effects which must be calibrated out. The spectral dynamic range depends on bandwidth in a poorly understood way. Applying the on-line autocorrelation bandpass correction only should result in about 50:1 dynamic range and is strongly discouraged. Values exceeding 10,000:1 at C and X-bands can be achieved but require careful data editing and bandpass calibration. A more typical limit is around 1000:1. L-band spectral dynamic ranges of $\sim 1000:1$ can be achieved by observing a suitable bandpass calibrator. Consult with Michael Rupen or another spectral line expert for more details.

Because the operational array currently consists of a mix of VLA and EVLA antennas, there are a number of additional complexities for spectral line observations. Some of these are listed below, but the cautious user should consult <http://www.vla.nrao.edu/astro/guides/evlareturn/> for a complete list.

Doppler tracking: Online Doppler tracking should be used only for projects employing only EVLA antennas, such as those making use of the extended EVLA tuning ranges. Online Doppler tracking should not be used if VLA-EVLA baselines are included in an experiment because of phase jumps on VLA-EVLA baselines introduced by the VLA Fluke synthesizers at any change in frequency or bandwidth. For the same reason, phase calibration must be included at any frequency or bandwidth change for observations using both VLA and EVLA antennas.

Closure errors: One may expect significant closure errors on VLA-EVLA baselines due

to their very different bandpasses; see Section 3.11 for more information.

Phase jumps and narrow bandpasses: The fine frequency tuning of the VLA is done by a set of “Fluke” synthesizers that may be set to an accuracy of 1 Hz. However, these synthesizers undergo frequent phase jumps when they are set to an accuracy better than 1 MHz (i.e., when any digits to the right of the decimal point are non-zero), and occasional phase jumps even for settings at integer numbers of megahertz. This has no impact on VLA-VLA baselines, since all antennas jump together. However, the EVLA antennas do not use the Fluke synthesizers, and do not undergo the frequent phase jumps, so VLA-EVLA baselines are compromised. We recommend that observers avoid the narrowest VLA spectral-line bandwidths (bandwidth codes 8 and 9; see Tables 18 and 19), and restrict their observing frequencies so that only multiples of 1 MHz are used for the fluke frequencies.⁶

Aliasing in narrow bandwidths: The hardware used to convert the digital signals from the EVLA antennas into analog signals to be fed into the VLA correlator causes power to be aliased into the bottom 0.5 MHz of baseband. This affects all sources with continuum emission, most notably, commonly-used gain calibrators. The aliased power is strongest at the very bottom of baseband, and decreases away from baseband. For all bands except X and U band on the VLA, the bottom of baseband is at low-numbered channels. For X and U band, the bottom of baseband occurs at high-numbered channels. This problem obviously affects the narrowest observing bandwidths the most, with bandwidth codes 6 (781 kHz total bandwidth, typically the narrowest commonly used on the VLA) and higher being affected over the full width of the band. Although we are investigating ways to mitigate this problem, it is likely that the effect will remain with us until the new EVLA correlator comes online. In fact, the problem will affect more and more baselines as more VLA antennas are retrofitted to EVLA antennas. Note that since the aliased signal does not correlate on VLA-EVLA baselines, only EVLA-EVLA baselines are affected.

3.16 VLBI Observations

The VLA often participates in VLBI observations with the VLBA, and in Global Network sessions which occur three or four times per year. The VLA supports VLBI observations in either single-antenna or phased-array modes. Data are recorded on a Mark 5A disk recording system after the single-antenna or phased-array data have been passed through the VLA’s VLBA data acquisition system. At this writing, we are just completing the implementation of phasing of the EVLA antennas together with the VLA antennas, so that the phased-array VLA will contain ~ 25 antennas added in phase rather than a maximum of ~ 20 . A comprehensive document entitled ‘VLBI at the VLA’ is available on the Web – point your browser to <http://www.vla.nrao.edu/astro/> and look under ‘Proposer Information and Documentation’. Be aware that this guide is somewhat out of date. **When the old VLA correlator is decommissioned at the beginning of 2010, it is possible that the software required for VLBI observing may not yet be enabled. Thus, there may be some period of time beginning in early 2010 when the EVLA cannot participate in VLBI observations.**

⁶Note that the phase jumps as a function of Fluke settings are still under investigation; please see <http://www.vla.nrao.edu/astro/guides/evlareturn/> for the latest information.

VLBI at the VLA is overseen by Amy Mioduszewski, who can be consulted for general information regarding matters such as phased-array or single-dish observations, or calibration of the VLA for VLBI. However, most VLBI projects involving the VLA, whether run during or outside of a Network session, will be assigned a DSOC contact by the Scheduler. Queries from an observer concerning specific information about a specific project should be directed to the DSOC contact assigned to the project. If the project's principal investigator or a co-investigator is an DSOC employee, then that person will be assumed to be the DSOC contact.

See Section 4.15 for information on absentee observing.

3.17 Snapshots

The two-dimensional geometry of the VLA allows a snapshot mode whereby short observations can be used to image relatively bright unconfused sources. This mode is ideal for survey work where the sensitivity requirements are modest. Due to confusion by background sources, use of snapshots is not recommended at 90 cm or 400 cm.

Single snapshots with good phase stability should give dynamic ranges of a few hundred. Note that because the snapshot synthesized beam contains high sidelobes, the effects of background confusing sources are much worse than for full syntheses, especially at 20 cm in the **D** configuration, for which a single snapshot will give a limiting noise of about 0.2 mJy. This level can be reduced by taking multiple snapshots separated by at least one hour. Use of the AIPS program **IMAGR** is necessary to remove the effects of background sources. Before considering snapshot observations at 20 cm, users should first determine if the goals desired can be achieved with the existing **FIRST** (**B** configuration) or **NVSS** (**D** configuration, all-sky) surveys. Both surveys can be accessed from the NRAO website, at: <http://www.vla.nrao.edu/astro/prop/largeprop/>.

3.18 Shadowing and Cross-Talk

Observations at low elevation in the **C** and **D** configurations will commonly be affected by shadowing. It is strongly recommended that all data from a shadowed antenna be discarded. This will automatically be done within the AIPS task **FILLM** when using the default inputs. Note that for versions of AIPS up through early incarnations of 31DEC01, **FILLM** is ignorant of antennas in other subarrays, or antennas which are out of the array, so flagging of antennas shadowed by antennas in other subarrays will not occur. For the final 31DEC01 AIPS and all subsequent versions, **FILLM** is smart enough to know about all antennas in all VLA subarrays.

Cross-talk is an effect in which signals from one antenna are picked up by an adjacent antenna, causing an erroneous correlation. At 20 cm, this effect is important principally in the **D** configuration. At 90 cm, **C** and even **B** configurations can also be affected. And at 400 cm, all configurations show strong cross-talk on many baselines. Careful editing is necessary to identify and remove this form of interference. For the 90 and 400 cm bands, use of the spectral line modes is strongly recommended to allow detection and removal of these contaminating signals.

3.19 Combining Configurations and Mosaicing

Any single VLA configuration will allow accurate imaging up to a scale approximately 30 times the synthesized beam. Objects larger than this will require multiple configuration

observations. For continuum projects, observers only need ensure that the frequencies used are similar for each configuration. It is not necessary that they be identical, but differences greater than 50 MHz could cause errors due to spectral index gradients. The different configurations may employ different bandwidths – indeed, this is often required to prevent bandwidth smearing (chromatic aberration). Objects larger than the primary antenna pattern may be mapped through the technique of interferometric mosaicing. Time-variable structures (such as the nuclei of radio galaxies and quasars) cause special, but manageable, problems. See the article by Mark Holdaway in reference 2 for more information.

3.20 Pulsar Observing

The hardware for pulsar-specific observing modes at the VLA is no longer supported, and potential proposers should consider making use of telescopes that are more suitable for pulsar timing observations. The VLA is most fruitfully used for pulsar observations in its more traditional observing modes, accepting the signal/noise penalty that is paid by accepting data at all times rather than gating the correlator synchronously with the pulsar. The EVLA will offer significant new pulsar observing capability with its new correlator, in 2011 or later.

3.21 Observing High Flux Density Sources – Special Corrections

The VLA correlator is a digital device, which causes a small but noticeable error in the calculation of the correlation coefficient when this coefficient is high. A recent change to the AIPS program FILLM now enables an approximate correction of this error when observations are taken in the continuum mode. Users may wish to apply this correction (commonly known as the ‘Van Vleck’ correction) when observing relatively unresolved objects with flux densities exceeding about 100 Jy (depending on band). Unfortunately, no correction for this effect for data taken in the spectral line modes is yet available.

3.22 Using VLA and EVLA Antennas Together

Throughout this document, we provide some specific information that may be essential for observing with the VLA while it combines both “old” VLA antennas and retrofitted EVLA antennas. However, since this document is updated only (approximately) annually, astronomers are urged to consult <http://www.vla.nrao.edu/astro/guides/evlareturn/> for the latest information, and follow the suggestions described therein. This is critical to the successful use of the VLA-EVLA baselines. The good news is that the ever-decreasing numbers of VLA antennas means that this will become less of an issue throughout 2009. Since the VLA antennas cannot be input to the EVLA correlator, the problems of EVLA-VLA baselines will disappear once the old VLA correlator is decommissioned in early 2010.

4 USING THE VLA

4.1 Obtaining Observing Time on the VLA

Observing time on the VLA is available to all researchers, regardless of nationality or location of institution. There are no quotas or reserved blocks of time. The allocation of observing time on the VLA is based upon the submission of a VLA Observing Proposal using the on-line VLA Proposal Submission Tool available via the NRAO Interactive Service

web page, at <http://my.nrao.edu/>. *Note that proposals using the old VLA L^AT_EX form are no longer accepted!* The on-line tool permits the detailed construction of a cover sheet specifying the requested observations, using a set of on-line forms, and uploading of a pdf-format scientific and technical justification to accompany the cover information.

It is also possible to receive VLA observing time by proposing to NASA missions, under cooperation agreements established between NRAO and those missions. Currently, such programs exist for the Chandra, Spitzer, and Fermi missions. Astronomers interested in those joint programs should consult the relevant mission proposal calls for more information.

Students planning to use the VLA for their Ph.D. dissertation may have a problem in that such dissertations are frequently composed of pieces of several short proposals which may not be suitable for combining into a single proposal for refereeing purposes. In this case, we shall accept, one per student, a ‘Plan of Dissertation Research’, of no more than 1000 words, at the time of the first proposal of the series, and which can be referred to in later proposals. The plan can be submitted via the NRAO Interactive Services webpage, at <http://my.nrao.edu/>. This provides some assurance against a dissertation being seriously damaged by adverse referee comments on one component proposal, when the referees may not see the whole picture. This facility is offered to students for which VLA observations are the most important component of their planned dissertations.

The VLA is scheduled on a trimester basis, with each trimester lasting four months. The proposal deadline for a particular configuration is 5PM (1700), Eastern Time on the 1st of February, June, or October which precedes the beginning of that configuration by three months or more. (If the first of the month falls on a Saturday or Sunday, the deadline is advanced to the next Monday.) As stated in Section 2, the traditional VLA configuration rotation will be modified beginning in January 2010. It is not necessary to submit a proposal at the last possible deadline for a particular configuration, since all proposals will be refereed immediately following the deadline of submission, regardless of the configuration requested. Early submissions (i.e., more than one deadline in advance of the relevant configuration deadline) will benefit from referee feedback and the opportunity for revision and additional review, if warranted.

All proposals are externally refereed by several experts in relevant subdisciplines (e.g. solar system, stellar, galactic, extragalactic, etc.). The referees’ comments and rating are strongly advisory to the VLA/VLBA Proposal Selection Committee, and the comments of both groups are passed on to the proposers soon after each meeting of the committee (three times yearly) and prior to the next proposal submission deadline. See <http://www.aoc.nrao.edu/epo/ad/scheduling.shtml> for a detailed description of the time allocation process.

Because of competition, even highly rated proposals are not guaranteed to receive observing time. This is particularly true for programs that concentrate on objects in the LST ranges occupied by popular targets such as the Galactic Center or the Virgo cluster. Daytime observing will also be limited by EVLA commissioning tests throughout 2009.

4.2 Rapid Response Science

The NRAO has established three categories of proposals for Rapid Response Science, which are described below and at <http://www.vla/nrao/edu/astro/prop/rapid/>. At present, Rapid Response Science is limited to a maximum of 5% of the total observing time on the VLA. All proposals for Rapid Response Science must be submitted using the standard NRAO procedures, using the on-line proposal tool. Proposals submitted by any other means

(e.g., phone calls, e-mails, faxes, word-of-mouth) will be rejected.

1. Known Transient Phenomena. These proposals will request time to observe phenomena that are predictable in general, but not in specific detail. For example, a proposal to observe the next flaring X-ray binary that meets certain criteria would be included in this category. Specific triggering criteria will be required. These proposals will be evaluated as part of the normal refereeing and scheduling process, and will be subject to the normal NRAO proposal deadlines. The proprietary period for observations of Known Transient Phenomena will be 12 months.

2. Exploratory Time. These proposals generally follow up on recent discoveries, with observations requested in advance of the period allocated at the most recent proposal deadline(s). Examples include **B** configuration proposals that follow up on **A** configuration discoveries made after the **B** configuration deadline, or a newly identified object that is a hot enough topic to warrant an image within a couple months. In general, there will not be a need for immediate scheduling with these proposals, but they may need to be observed in the current VLA configuration rather than waiting 16 months. Proposals for Exploratory Time will be evaluated by a subset of the VLA/VLBA Proposal Selection Committee, and may or may not be sent to external referees. The possibility that a proposer forgets about or misses a proposal deadline will not constitute sufficient justification for granting of observing time by this process. Notification of the dispensation of Exploratory Time proposals normally will be within two weeks of reception of the proposal; most of the accepted proposals are placed in the dynamic scheduling queue, and are not guaranteed to be observed. The proprietary period for Exploratory Time will be six months.

3. Target of Opportunity. These proposals are for true targets of opportunity—unexpected or unpredicted phenomena such as supernovae, novae, or extreme X-ray, optical, or radio flares in various types of objects. These proposals will be evaluated rapidly, with scheduling done as quickly as possible and as warranted by the nature of the transient phenomenon. Notification of the dispensation of Target of Opportunity proposals will always be within two weeks, and may be much faster, depending on the requirements of the proposed observation. The proprietary period for Targets of Opportunity will be decided on a case-by-case basis, and will in no instances be longer than six months.

4.3 Data Analysts and General Assistance

General assistance of all kinds is available through the data analysts. They can be considered to be advocates for all VLA users, and should be consulted first when you encounter any problem. Note that they are not available to perform remote data calibration. The e-mail address for all the data analysts is: analysts@nrao.edu.

4.4 Observing File Preparation

To use the VLA, an observing file must be prepared and submitted to VLA Operations. This file may be generated by the NRAO-supplied program `JObserve`, which is a GUI-based version of the older `OBSERVE` program, offering a more modern graphical user interface without `OBSERVE`'s keypad mapping problems. Some new capabilities have been added to `JObserve` only.

After your file is prepared, e-mail it to the operators at observe@nrao.edu. Include the program name in the subject line. The operators always acknowledge receipt of the observing file by e-mail. If you do not receive a timely response, call the telescope operators

at 575-835-7180. Please complete these operations at least two working days before your observing.

JObserve distributions are currently available for Solaris (Sparc) and Linux with instructions provided to allow a user to port one of these distributions to any machine which can run the Java 2 runtime environment. The latest version of JObserve is 1.7.4, released January 13, 2006, and it may be downloaded from <http://www.aoc.nrao.edu/software/jobserve/>.

In 2009, the first version of a new “Observation Preparation Tool,” or OPT, will become available for the EVLA. The OPT will be necessary to set up any observations at the new observing band of 1.0 cm (26.5–40 GHz), which is expected to become available in mid-year.

4.5 Fixed Date and Dynamic Scheduling

Most of the observing time on the VLA is allocated as “fixed-time” observing, with the observer being given a particular sidereal date and time allocation on the VLA. However, the VLA gradually is moving toward a system in which more observations are scheduled dynamically, based on a combination of scientific priority and the expected properties of the array and the weather. In particular, all time during antenna moves and all “filler” time are scheduled dynamically. The procedure for generating observing scripts is similar to that described in Section 4.4, except that the individual scans must be specified in time durations rather than by the absolute stop time. After preparation, observe files for dynamic scheduling are e-mailed to dynsoc@nrao.edu for queueing. Since the details of dynamic scheduling are changing on a more frequent basis than this document, we refer the reader to the scheduling officers’ home page for further information; this page is located at <http://www.aoc.nrao.edu/~schedsoc/>.

4.6 The Observations and Remote Observing

Observers need not be present at the VLA to obtain VLA data. However, we encourage VLA users to come to Socorro when observing. There is no better way to interact with the data, and to calibrate and image data quickly. And coming to Socorro is the best way to benefit from discussions with staff members.

We recommend that observers who are coming to Socorro, and who intend to set up their observing files there, arrive two working days before their scheduled observations to allow sufficient time to interact with key staff members. See Section 4.12 for information on coming to and staying in Socorro.

For those who choose to process their data at home, the data can be retrieved from the VLA on-line archive after obtaining the project key from the data analysts, or by using the NRAO Interactive Services login from the archive web page. Alternatively, the data analysts will, upon request, mail you a tape (Exabyte or DAT) containing your uncalibrated data in its original format. The AIPS task FILLM is used to load these data to disk.

4.7 Data Processing

NRAO supports the AIPS (Astronomical Image Processing System) software as its primary data-analysis package for the VLA. This portable package may be run under various flavors of Linux or Unix operating systems, as well as Mac-OS. Most observers install and use the software on their desktop computers and/or laptops to reduce their VLA data. See <http://www.aoc.nrao.edu/aips/> for more details.

NRAO is presently developing the CASA (Common Astronomy Software Applications) package, primarily for data analysis using the EVLA and ALMA. CASA is currently undergoing beta testing and is available upon request. See <http://casa.nrao.edu> for more information.

4.8 Travel Support for Visiting the DSOC and VLA

For each observing program scheduled on an NRAO telescope, reimbursement may be requested for one of the investigators from a U.S. institution to travel to the NRAO to observe, and for one U.S.-based investigator to travel to the NRAO to reduce data. Reimbursement may be requested for a second U.S.-based investigator to either observe or reduce data provided the second investigator is a student, graduate or undergraduate. In addition, the NRAO will, in some cases, provide travel support to the Observatory for research on archival data. The reimbursement will be for the actual cost of economy airfare, up to a limit of \$1000, originating from within the U.S. including its territories and Puerto Rico. Costs of lodging in NRAO facilities can be waived on request in advance and with the approval of the relevant site director. No reimbursement will be made for ground transportation or meals.

To qualify, the U.S. investigator must not be employed at a Federally Funded Research and Development Center (FFRDC) or its sponsoring agency. The NSF maintains a master government list of some FFRDCs at <http://www.nsf.gov/statistics/nsf06316/>.

To claim this reimbursement, obtain an expense voucher from Lori Appel in the Assistant Director's office in the DSOC.

4.9 Student Assistance for Data Reduction Visits to the DSOC

Students visiting the Array Operation Center for the purposes of working on a VLA or VLBA observing program may be eligible to have their lodging expenses in the NRAO guest house covered by NRAO. To qualify, the student must be a graduate or undergraduate enrolled at a University in the U.S., working on an approved observing program. These are the same qualifications as required for NRAO support of air travel costs described above. In addition, the duration of the visit should be between 5 and 30 days. Requests for support should be made to Claire Chandler at least 4 weeks in advance of the proposed visit. If this is a first time visit then the student should be accompanied by a collaborator on the project, or alternatively an NRAO collaborator may be requested.

4.10 Real-Time Observing

A workstation, connected to the on-line computers by an Ethernet link, is now in place at the VLA site. A special version of the AIPS task FILLM will fill VLA data into this workstation's disks in real time. Each scan is available for editing, calibration, and imaging with AIPS within a few seconds of the end of that scan. Data also can be written to a local Exabyte tape.

The real-time data pipeline also has been extended to the DSOC. Any workstation at the DSOC can now receive VLA data as it is produced. However, this capacity is not available beyond the DSOC.

4.11 Computing at the DSOC

A primary goal of the computing environment at the DSOC is to allow every user full access to a workstation during his/her visit. There are 8 public workstations available at the DSOC for full-time data reduction by visitors. They are mostly four-processor, 2.0-GHz PCs running Linux.

For hardcopy, we have a number of high volume B&W laser printers, two color Postscript laser printers which can reproduce on both paper and transparencies, and one wide-bed color printer.

Visitors may reserve time on these workstations when they make their travel arrangements with the Reservationist (see Section 4.12). The reservationist's e-mail is: nmreserv@nrao.edu.

If you require computing assistance while at the DSOC, contact the help desk (e-mail to helpdesk@aac.nrao.edu, extension 7213, office 262).

For a more complete description of computing facilities at the DSOC, see <http://www.aoc.nrao.edu/computing/>.

4.12 Reservations for VLA and/or DSOC

Advance contact with the Reservationist (nmreserv@nrao.edu) at least 1 week prior to your visit to the NRAO/NM is required, and 2 weeks' notice is preferred, in order to optimize the logistics of room occupancy, transportation, computer load, and staff assistance. You may now book your visit to the DSOC through the WWW. From the NRAO home page, press the 'Astronomers' link, then 'VLA/EVLA', then 'Visit Array Operations Center (AOC) Website', then 'Official Visitors', and finally the 'Visitor's Registration Form' link.

First-time visiting students will be allowed to come to the NRAO/NM for observations or data reduction only if they are accompanied by their faculty advisor, or if they have a collaborating NRAO staff member.

4.13 Staying in Socorro

Visitors to Socorro can take advantage of the NRAO Guest House. This facility contains eight single, four double, and two two-bedroom apartments, plus a lounge/kitchen, and full laundry facilities. The Guest House is located on the New Mexico Tech (NMIMT) campus, a short walk from the DSOC. Reservations are made through the Reservationist (nmreserv@nrao.edu.)

4.14 Help for Visitors to the VLA and DSOC

We encourage observers to come to Socorro to calibrate and image their data. This is the best way to ensure the quickest turnaround and the best results from their observing. While in Socorro, each observer will interact with members of the DSOC staff in accordance with his/her level of experience and the complexity of the observing program. If requested on the original VLA application form, the visiting observer will be guided through the steps of data calibration and imaging by a prearranged staff friend or scientific collaborator. A list of staff scientists and their interests can be found at <http://www.aoc.nrao.edu/epo/AD/aoc-research.html>. The data analysts and the computer operations staff are also available for consultation on AIPS procedures and systems questions.

4.15 VLBI Remote Observing

The VLA supports absentee VLBI observations, whether conducted during, or outside of, a Global Network session. Queries from an absentee observer concerning a specific project should be directed to the DSOC contact assigned to that project (see Section 3.16). VLA schedule file preparation assistance is provided by the data analysts (see Section 4.3). Absentee observers must provide the data analysts with all necessary scheduling information. For a Network project, this information is due at least two weeks before the start of the appropriate Network session. For a non-Network project, this information is due by the schedule file due date assigned by the VLBA scheduler.

Although VLA Operations fully supports absentee VLBI observing, visits by observers are welcomed and are especially encouraged if the observations are in any way atypical. Included in this category are VLBI spectral line projects regardless of recording format, and any phased-array VLBI projects for which radio frequency interference is expected.

For more information, consult ‘VLBI at the VLA’, at <http://www.vla.nrao.edu/astro/guides/vlbivla/current/>.

4.16 On-Line Information about the NRAO and the VLA

NRAO-wide information is available on the World Wide Web through your favorite Web browser at URL <http://www.nrao.edu>, and information specific to astronomers using the VLA may be found at <http://www.vla.nrao.edu/astro/>. We strongly recommend usage of this on-line service, which is regularly updated by the NRAO staff.

5 MISCELLANEOUS

5.1 VLA Archive Data

The VLA archive contains all VLA data since observing started in 1976. The entire archive is now on disk, and is available via the web. A catalog describing these observations can be accessed from <http://archive.nrao.edu/archive/>. Data-base searches may be made based on a large number of user-specified criteria, and automatic downloading of the data via standard ftp protocols. With the exception of some rapid response and large proposals, VLA data associated with a given proposal normally are restricted to proprietary use by the proposing team for a period of 12 months from the date of the last observation in a proposal.⁷ Proprietary data may be downloaded by the observing team by making use of the project key (see Section 4.6).

5.2 Publication Guidelines

5.2.1 Acknowledgement to NRAO

Any papers using observational material taken with NRAO instruments (VLA or otherwise) or papers where a significant portion of the work was done at NRAO, should include the following acknowledgement to NRAO and NSF:

⁷Data taken more than 12 months previously may still be proprietary, if additional data for the same proposal have been taken within the last 12 months.

The National Radio Astronomy Observatory is a facility of the National Science Foundation operated under cooperative agreement by Associated Universities, Inc.

5.2.2 Dissertations

Students whose dissertations include observations made with NRAO instruments are expected to provide copies of, or links to, their theses for inclusion and maintenance at the NRAO library. These will be catalogued and made available via the NRAO library catalogue. If a paper copy (unbound is acceptable), it may be submitted to the DSOC Librarian who will send it to Charlottesville for cataloguing.

5.2.3 Preprints

NRAO requests that you submit the `astro-ph` link or an electronic copy of any accepted papers that include observations taken with any NRAO instrument or have NRAO author(s) to the Observatory Librarian. For further information, contact the Librarian in Charlottesville (`library@nrao.edu`) or read the instructions on the web page at <http://www.nrao.edu/library/preprints.shtml>.

5.2.4 Reprints

Given the prevalence of electronic access to the literature, NRAO will no longer pay for the purchase of reprints of published papers.

5.2.5 Page Charge Support

The following URL contains complete information on the observatory's policy regarding page charge support: http://www.cv.nrao.edu/library/page_charges.html. The following is a summary:

- When requested, NRAO will pay the larger of the following:
 - 100% of the page charge share for authors at a U.S. scientific or educational institute reporting original results made with NRAO instrument(s). See the VLA web pages for more details.
 - 100% of the page charge share for NRAO staff members.
- Page charge support is provided for publication of color plates.
- To receive page charge support, authors must comply with all of the following requirements:
 - Include the NRAO footnote in the text (see Section 5.2.1).
 - Send the `astro-ph` link or an electronic copy of the paper upon acceptance or posting on `astro-ph` to the Observatory Librarian (`library@nrao.edu`), with the request for page charge support. The Librarian will respond with the amount covered (based on the NRAO page charge policy) and will request the page charge form, with manuscript information completed, via fax (434-296-0278) or e-mail (`library@nrao.edu`). For questions, contact the Observatory Librarian at 434-296-0254.

6 DOCUMENTATION

Documentation for VLA data reduction, image making, observing preparation, etc., can be found in various manuals. Most current manuals are available on-line via the World Wide Web (see Section 4.16). Those manuals marked by an asterisk (*) can be mailed out upon request, or are available for downloading from the NRAO website. Direct your requests for mailed hardcopy to Lori Appel. Many other documents of interest to the VLA user, not listed here, are available from our website.

1. PROCEEDINGS FROM THE 1988 SYNTHESIS IMAGING WORKSHOP: Synthesis theory, technical information and observing strategies can be found in: ‘Synthesis Imaging in Radio Astronomy’. This collection of lectures given in Socorro in June 1988 has been published by the Astronomical Society of the Pacific as Volume 6 of their Conference Series.
2. PROCEEDINGS FROM THE 1998 SYNTHESIS IMAGING WORKSHOP: This is an updated and expanded version of Reference 1, taken from the 1998 Synthesis Imaging Summer School, held in Socorro in June, 1998. These proceedings are published as Volume 180 of the ASP Conference Series.
3. INTRODUCTION TO THE NRAO VERY LARGE ARRAY (Green Book): This manual has general introductory information on the VLA. Topics include theory of interferometry, hardware descriptions, observing preparation, data reduction, image making and display. Major sections of this 1983 manual are now out of date, but it nevertheless remains the best source of information on much of the VLA. Copies of this are found at the VLA and in the DSOC, but no new copies are available. Much of this document is available for downloading through the NRAO’s website.
4. *A SHORT GUIDE FOR VLA SPECTRAL LINE OBSERVERS: This is an important document for those wishing to carry out spectral- line observations with the VLA. The revised, 1995 version is still fairly current.
5. *AIPS COOKBOOK: The ‘Cookbook’ description for calibration and imaging under the AIPS system can be found near all public workstations in the DSOC. The latest version has expanded descriptions of data calibration imaging, cleaning, self- calibration, spectral line reduction, and VLBI reductions. See <http://www.aoc.nrao.edu/aips/cook.html>.
6. *GOING AIPS: This is a two-volume programmers manual for those wishing to write programs under AIPS. It is now somewhat out of date. See <http://www.aoc.nrao.edu/aips/aipsdoc.html#GOAIPS>.
7. *VLA CALIBRATOR MANUAL: This manual contains the list of VLA Calibrators in both 1950 and J2000 epoch and a discussion of gain and phase calibration, and polarization calibration. See <http://www.vla.nrao.edu/astro/calib/manual/>.
8. *VLBI AT THE VLA. Everything you ever wanted to know about VLBI at the VLA. Somewhat out of date. See <http://www.vla.nrao.edu/astro/guides/vlbivla/current/>.
9. *The Very Large Array: Design and Performance of a Modern Synthesis Radio Telescope, Napier, Thompson, and Ekers, Proc. of IEEE, 71, 295, 1983.

10. *OBSERVE, A GUIDE FOR SPECTRAL LINE OBSERVERS. A tutorial manual for observers, with special emphasis on spectral line applications.
11. *HIGH FREQUENCY OBSERVING GUIDE. A web-based manual with a great deal of information for users about observing with the VLA 0.7 cm and 1.3 cm observing systems. See <http://www.vla.nrao.edu/astro/guides/highfreq/>.
12. *VLA MEMO SERIES. See <http://www.vla.nrao.edu/memos/>.
13. *EVLA MEMO SERIES. See <http://www.aoc.nrao.edu/evla/memolist.shtml>.

7 KEY PERSONNEL

Table 20 gives the telephone extensions and DSOC room numbers of personnel who are available to assist VLA users. In most cases the individuals have responsibilities or special knowledge in certain areas as noted in the right hand column. You also may contact any of these people through E-mail, as noted at the end of the table.

8 Acknowledgments

Over the VLA history of more than 25 years, many individuals have contributed to this document by writing sections, editing previous versions, commenting on draft material, and implementing the capabilities described herein. We thank all these contributors for their efforts. The listed editors of the present version of this document are the editors of the most recent versions, and thus are the best individuals for readers to contact if they should have questions on the material, or suggestions that would enhance the clarity of this guide.

Table 20: **Key VLA Personnel**

Name	Phone	Room	Notes
Lori Appel	7310	340	Scheduling administrator, AD office
John Benson	7399	366	Data archive
Sanjay Bhatnagar	7376	309	CASA; Imaging algorithms
Walter Brisken	7133	373	Pulsars; EVLA calibration
Bryan Butler	7261	344	EVLA Computing Division Head; VLA high frequencies
Chris Carilli	7306	356	NRAO Chief Scientist; VLA high frequencies
Claire Chandler	7365	328	Deputy AD for Science; VLA high frequencies
Barry Clark	7268	308	VLA/VLBA scheduling
Mark Claussen	7284	268	VLA user support; VLA scheduling
Vivek Dhawan	7378	310	EVLA commissioning
Bob Dickman	7300	336	VLA/VLBA Assistant Director
Dale Frail	7338	332	NRAO Assistant Director for Science & Academic Affairs
Miller Goss	7267	332	Spectral line
Eric Greisen	7236	318	AIPS
Helpdesk	7213	262	Computer Helpdesk
Leonid Kogan	7383	312	AIPS
Mark McKinnon	7273	326	EVLA Project Manager
Dan Mertely	7128	VLA-128	RFI monitoring and mitigation
Amy Mioduszewski	7263	208	AIPS; VLA calibrator models; VLBI at the VLA
George Moellenbrock	7406	368	CASA; polarimetry
Emmanuel Momjian	7452	301	EVLA commissioning
Steve Myers	7294	376	VLA calibration; polarimetry; CASA Project Scientist
Frazer Owen	7304	320	High dynamic range; wide-field imaging
Peggy Perley	7214	282	Deputy Assistant Director for Operations
Rick Perley	7312	362	EVLA Project Scientist; flux calibration
Receptionist	7300	Front	DSOC receptionist; aocrecep@nrao.edu
Reservationist	7357	218	DSOC reservations; nmreserv@nrao.edu
James Robnett	7226	258	Computing Infrastructure Division Head
Michael Rupen	7248	206	EVLA scientific software; spectral line
Debra Shepherd	7398	266	Mosaicing
Lorant Sjouwerman	7332	367	VLA Pipeline
Ken Sowinski	7299	375	On-line systems
Meri Stanley	7238	204	Lead data analyst
Jim Ulvestad	Lead editor of this document
Gustaaf van Moorsel	7396	348	User support
VLA Operator	7180	VLA	On-duty VLA Operator
VLBA Operator	7251	269	On-duty VLBA Operator
Stephan Witz	7335	316	JObserve
Joan Wrobel	7392	302	VLA/VLBA scheduling
Wes Young	7337	378	Real-time observing

Note: You may e-mail any of the above individuals by addressing your message to ‘first initial last name’@nrao.edu. Thus, you may contact Joanne Astronomer at: ‘jastrono@nrao.edu’. The name is truncated to eight characters. For contact with the AIPS software group, please e-mail “daip@nrao.edu”. For questions about telescope time allocation, please e-mail “schedsoc@nrao.edu”. The listed four-digit numbers are sufficient for calls made from within the DSOC. If you are calling from the U.S. or Canada, the 4-digit numbers must be preceded with: 1-575-835 from landlines, or 575-835 with mobile phones. (Note that the area code for the VLA site and the DSOC changed from ‘505’ to ‘575’ in 2007; calls using the old area code will no longer be connected.) If you are calling from outside the U.S. or Canada, the 4-digit numbers must be preceded with 1-575-835.